

4

TECHNICAL REPORT BRL-TR-3029

BRL

A WORKSHOP SUMMARY OF
MODEL PREDICTIONS OF THE PISTON-DRIVEN-COMPACTION
EXPERIMENT"

DOUGLAS E. KOOKER

AUGUST 1989

DTIC
ELECTE
OCT 12 1989
S B D

APPROVED FOR PUBLIC RELEASE; DISTRIBUTION UNLIMITED.

U.S. ARMY LABORATORY COMMAND

BALLISTIC RESEARCH LABORATORY
ABERDEEN PROVING GROUND, MARYLAND

AD-A213 330

89 10 12 028

DESTRUCTION NOTICE

Destroy this report when it is no longer needed. DO NOT return it to the originator.

Additional copies of this report may be obtained from the National Technical Information Service, U.S. Department of Commerce, Springfield, VA 22161.

The findings of this report are not to be construed as an official Department of the Army position, unless so designated by other authorized documents.

The use of trade names or manufacturers' names in this report does not constitute indorsement of any commercial product.

UNCLASSIFIED

SECURITY CLASSIFICATION OF THIS PAGE

Form Approved
OMB No. 0704-0188

REPORT DOCUMENTATION PAGE

1a. REPORT SECURITY CLASSIFICATION Unclassified			1b. RESTRICTIVE MARKINGS		
2a. SECURITY CLASSIFICATION AUTHORITY			3. DISTRIBUTION/AVAILABILITY OF REPORT APPROVED FOR PUBLIC RELEASE; DISTRIBUTION UNLIMITED		
2b. DECLASSIFICATION/DOWNGRADING SCHEDULE			4. PERFORMING ORGANIZATION REPORT NUMBER(S) BRL-TR-3029		
4. PERFORMING ORGANIZATION REPORT NUMBER(S) BRL-TR-3029			5. MONITORING ORGANIZATION REPORT NUMBER(S)		
6a. NAME OF PERFORMING ORGANIZATION US Army Ballistic Research Laboratory		6b. OFFICE SYMBOL (if applicable) SLCBR-IB-I	7a. NAME OF MONITORING ORGANIZATION		
6c. ADDRESS (City, State, and ZIP Code) Aberdeen Proving Ground, MD 21005-5066			7b. ADDRESS (City, State, and ZIP Code)		
8a. NAME OF FUNDING/SPONSORING ORGANIZATION NSWC / White Oak		8b. OFFICE SYMBOL (if applicable) R-10F	9. PROCUREMENT INSTRUMENT IDENTIFICATION NUMBER		
8c. ADDRESS (City, State, and ZIP Code) 10901 New Hampshire Ave. Silver Spring, MD 20903-5000			10. SOURCE OF FUNDING NUMBERS	PROGRAM ELEMENT NO. 64363N	PROJECT NO. J0951
10901 New Hampshire Ave. Silver Spring, MD 20903-5000			TASK NO. J0951	WORK UNIT ACCESSION NO.	
11. TITLE (Include Security Classification) A WORKSHOP SUMMARY OF "MODEL PREDICTIONS OF THE PISTON-DRIVEN-COMPACTION EXPERIMENT"					
12. PERSONAL AUTHOR(S) Douglas E. Kooker					
13a. TYPE OF REPORT Technical Report		13b. TIME COVERED FROM June 1988 to Mar 1989	14. DATE OF REPORT (Year, Month, Day)		15. PAGE COUNT
16. SUPPLEMENTARY NOTATION					
17. COSATI CODES			18. SUBJECT TERMS (Continue on reverse if necessary and identify by block number)		
FIELD	GROUP	SUB-GROUP			
21	02		Granular Explosives/Propellants; Impact; Compaction Waves;		
20	14		Modeling; Combustion/Deflagration; Transition to Detonation		
19. ABSTRACT (Continue on reverse if necessary and identify by block number) <p>A JANNAF Propulsion Systems Hazards Subcommittee Workshop was held on 25-26 October 1988 in conjunction with the 25th JANNAF Combustion Meeting in Huntsville, AL. The area of interest is the transition to detonation in confined granular energetic material. This workshop focused on the acceleration of a strong compaction wave, before the onset of detonation. The objective was to compare model predictions to four Piston-Driven-Compaction experiments involving two different ball propellants. These were true predictions, since the experimental data were not released until the second day of the workshop. Several of the models came close to the compaction wave locus. However, it was more difficult to predict wall stress time-history seen by two transducers at fixed locations along the tube. The timing of a "runaway" is extremely sensitive to the intense competition among sources of reaction and heat loss.</p>					
20. DISTRIBUTION/AVAILABILITY OF ABSTRACT <input type="checkbox"/> UNCLASSIFIED/UNLIMITED <input checked="" type="checkbox"/> SAME AS RPT. <input type="checkbox"/> DTIC USERS			21. ABSTRACT SECURITY CLASSIFICATION Unclassified		
22a. NAME OF RESPONSIBLE INDIVIDUAL Douglas E. Kooker			22b. TELEPHONE (Include Area Code) (301) 278-6101	22c. OFFICE SYMBOL SLCBR-IB-I	

CONTENTS

	<u>Page</u>
LIST OF FIGURES.....	5
LIST OF TABLES.....	7
I. INTRODUCTION.....	9
II. PROBLEM DESCRIPTION.....	11
Information Supplied to Modelers.....	12
(A) From the PDC Experiment.....	12
(B) Quasi-Static Compaction Data.....	13
(C) Propellant Ignition and Burning Rate Data.....	13
(D) Compressibility of TMD Propellant.....	13
III. DISCUSSION OF RESULTS.....	14
PDC-80 (Problem #1).....	15
PDC-81 (Problem #2).....	19
PDC-82 (Problem #3).....	19
PDC-M30 (Problem #4).....	26
IV. CONCLUDING REMARKS.....	26
ACKNOWLEDGEMENTS.....	29
REFERENCES.....	31
APPENDIX - SCHEMATIC DESCRIPTIONS OF MODELS.....	33
DISTRIBUTION LIST.....	39

Accession For		
NTIS GRA&I	<input checked="" type="checkbox"/>	
DTIC TAB	<input type="checkbox"/>	
Unannounced	<input type="checkbox"/>	
Justification		
By _____		
Distribution/ _____		
Availability Codes		
Dist	Avail and/or	Special
A-1		

LIST OF FIGURES

<u>Figure</u>	<u>Page</u>
1	Schematic of Modeling Problem and NSWC Experiment [3]10
2a	Compaction Wave Locus for PDC-80 (Problem #1); 160 m/s Impact on 60.2% TMD TS-3659. Tube Length is 101.7 mm. Experimental Data from Sandusky et. al. [3].....16
2b	Compaction Wave Locus for PDC-80 (Problem #1); 160 m/s Impact on 60.2% TMD TS-3659. Comparison of Workshop Predictions with Data from Sandusky et. al. [3].....16
3a	Time-History From Wall-Mounted Transducers for PDC-80 (Problem #1); 160 m/s Impact on 60.2% TMD TS-3659. Experimental Data from Sandusky et. al. [3]. Gage #1 is Located at 38.1 mm, and Gage #2 at 76.2 mm; Tube Length is 101.7 mm.....17
3b	Time-History From Wall-Mounted Transducers for PDC-80 (Problem #1); 160 m/s Impact on 60.2% TMD TS-3659. Comparison of Workshop Predictions with Data from Sandusky et. al. [3]. Gage #1 is Located at 38.1 mm, and Gage #2 at 76.2 mm; Tube Length is 101.7 mm.....17
4a	Compaction Wave Locus for PDC-81 (Problem #2); 237 m/s Impact on 60.1% TMD TS-3659. Tube Length is 146.8 mm. Experimental Data of Sandusky et. al. [3].....20
4b	Compaction Wave Locus for PDC-81 (Problem #2); 237 m/s Impact on 60.1% TMD TS-3659. Comparison of Workshop Predictions with Microwave Data from Sandusky et. al. [3].....20
5a	Time-History From Wall-Mounted Transducers for PDC-81 (Problem #2); 237 m/s Impact on 60.1% TMD TS-3659. Experimental Data from Sandusky et. al. [3]. Gage #1 is Located at 38.1 mm, and Gage #2 at 76.2 mm; Tube Length is 146.8 mm.....21
5b	Time-History From Wall-Mounted Transducers for PDC-81 (Problem #2); 237 m/s Impact on 60.1% TMD TS-3659. Comparison of Workshop Predictions with Data from Sandusky et. al. [3]. Gage #1 is Located at 38.1 mm, and Gage #2 at 76.2 mm; Tube Length is 146.8 mm.....21
6a	Compaction Wave Locus for PDC-82 (Problem #3); 300 m/s Impact on 60.1% TMD TS-3659. Tube Length is 146.8 mm. Experimental Data of Sandusky et. al. [3].....22
6b	Compaction Wave Locus for PDC-82 (Problem #3); 300 m/s Impact on 60.1% TMD TS-3659. Comparison of Workshop Predictions with Microwave Data from Sandusky et. al. [3].....22

Figure

Page

7a Time-History From Wall-Mounted Transducers for PDC-82 (Problem #3); 300 m/s Impact on 60.1% TMD TS-3659. Experimental Data from Sandusky et. al. [3]. Gage #1 is Located at 38.1 mm, and Gage #2 at 76.2 mm; Tube Length is 146.8 mm.....23

7b Time-History From Wall-Mounted Transducers for PDC-82 (Problem #3); 300 m/s Impact on 60.1% TMD TS-3659. Comparison of Workshop Predictions with Data from Sandusky et. al. [3]. Gage #1 is Located at 38.1 mm, and Gage #2 at 76.2 mm; Tube Length is 146.8 mm.....23

8a Compaction Wave Locus for PDC-M30 (Problem #4); 210 m/s Impact on 60.5% TMD WC-140. Tube Length is 146.8 mm. Experimental Data from Sandusky et. al. [3].....24

8b Compaction Wave Locus for PDC-M30 (Problem #4); 210 m/s Impact on 60.5% TMD WC-140. Comparison of Workshop Predictions with Microwave Data from Sandusky et. al. [3].....24

9a Time-History From Wall-Mounted Transducers for PDC-M30 (Problem #4); 210 m/s Impact on 60.5% TMD WC-140. Experimental Data from Sandusky et. al. [3]. Gage #1 is Located at 38.1 mm, and Gage #2 at 76.2 mm; Tube Length is 146.8 mm.....25

9b Time-History From Wall-Mounted Transducers for PDC-M30 (Problem #4); 210 m/s Impact on 60.5% TMD WC-140. Comparison of Workshop Predictions with Data from Sandusky et. al. [3]. Gage #1 is Located at 38.1 mm, and Gage #2 at 76.2 mm; Tube Length is 146.8 mm.....25

10 Time-History From Wall-Mounted Transducers for PDC-M30 (Problem #4); 210 m/s Impact on 60.5% TMD WC-140. Comparison of Workshop Predictions with Data from Sandusky et. al. [3]. Scale to Illustrate Low Level Gage Response.....27

11 Time-History From Wall-Mounted Transducers for PDC-M30 (Problem #4); 210 m/s Impact on 60.5% TMD WC-140. Comparison of Workshop Predictions From Weston with Data from Sandusky et. al. [3]. Gage #1 is Located at 38.1 mm, and Gage #2 at 76.2 mm; Tube Length is 146.8 mm.....27

LIST OF TABLES

Table	Page
I Propellant Properties.....	11
II Initial Conditions for PDC Modeling Problems.....	12
III Summary of Contributions.....	14

I. INTRODUCTION

The JANNAF Propulsion Systems Hazards Subcommittee sponsored a Workshop entitled "Model Predictions of the Piston-Driven-Compaction Experiment" which was held on 25-26 October 1988 in conjunction with the 25th JANNAF Combustion Meeting at NASA/Marshall Space Flight Center, Huntsville, AL. The general problem of interest is the transition to detonation in confined granular energetic material. This workshop is the third in a series of JANNAF PSHS workshops which have attempted to examine various aspects of the problem. The first one was held on 11-12 July 1985 in the Albuquerque Convention Center, Albuquerque NM, immediately preceding the Eighth Symposium (International) on Detonation, 15-19 July 1985. The objective was to assess our knowledge (or ignorance) of the mechanical properties exhibited by compacted granular material. Discussion concentrated on quasi-static compaction, as well as dynamic compaction and small amplitude wave propagation which may involve strain rate effects. Reference [1] is the workshop summary.

The second workshop was held on 23 October 1986 at the NASA / Langley Research Center in Hampton VA, in conjunction with the 23rd JANNAF Combustion Meeting, 20-24 October 1986. The specific objective was to gather eight modelers together and compare predictions to three pre-assigned "homework" problems which were based on constant-velocity-piston compaction of a column of confined granular material. The broader objective was an elementary assessment of the predictive capability of a number of computer codes used in the modeling of Deflagration-to-Detonation Transition (DDT). Of course, success in predicting compaction wave speed is only a necessary condition and not sufficient proof that a DDT prediction will be accurate. The good news from this workshop was that most of the predictions were close to each other and to the "correct" answers which were taken from experimental compaction wave speed data obtained by H. W. Sandusky (NSWC/WO) in his Piston-Driven-Compaction (PDC) apparatus. The bad news was that compaction wave speed is a rather forgiving parameter; models which predict nearly the same wave speed were observed to predict different values of pressure (or stress) in the aggregate. It was concluded that on the basis of compaction wave speed, there is no way to distinguish the influence of (a) strain-rate sensitivity during dynamic compaction, (b) compaction wave-induced reaction of solid material, and (c) friction between the sliding aggregate and the wall boundary. Reference [2] is the workshop summary.

The current workshop (Oct 1988) is an attempt to confront a problem closer to "transition", without requiring computations of a full high order detonation. The aim is to focus on wave behavior in the "intermediate regime", as the strong compaction wave accelerates to speeds in the range of low velocity detonation. When constructing a modeling exercise which is to predict the behavior of an experiment, an absolute necessity is the ability to uniquely specify the boundary conditions and/or source terms which drive the problem. If the problem is posed such that various combinations of boundary values and source terms could be selected as reasonable, then comparison of model predictions will be meaningless. This is the difficulty associated with experiments based on convective ignition - specifying the spatial distribution and time-history of mass flux and energy content of the ignitor system. It was felt that Sandusky's PDC experiment should not suffer from this ambiguity; the experimental values of projectile location as a function of time would provide a unique time-dependent boundary condition for the models. Different initial wave strengths could be generated by varying the initial speed of the projectile. However, the original PDC experiment

would have to be modified by the addition of one or more pressure transducers at fixed locations along the tube length. These would provide time-history of stress in the compacted aggregate as the event developed, and help distinguish among various model predictions. Thus, the current workshop extends the theme of the Oct 1986 workshop [2] to a more difficult problem.

A novel aspect of the current workshop is that the modelers were asked to make true predictions, not just simulate known data. Although the PDC experiments were run in advance, the results were not released until the second day of the workshop. Thus all the modelers (including the chairman) were "blind". Approximately four months in advance, each modeler was given the initial conditions, the time-dependent boundary condition, and properties of the granular propellant. There were four experiments involving two different materials. The modeler was asked to predict the compaction wave locus, and the stress time-history which would be seen by gages at two fixed locations in the chamber. Six individuals agreed to be subjected to this torture, and five brought predictions to the Workshop. They were:

- M. R. Baer, Sandia National Laboratory / Albuquerque
- K. Kim and T. Hsieh, Naval Surface Warfare Center / White Oak Laboratory
- D. E. Kooker, U. S. Army Ballistic Research Laboratory
- C. F. Price, Naval Weapons Center / China Lake
- A. M. Weston, Brobeck Corp / Lawrence Livermore National Laboratory

The first day of the workshop was devoted to presentation of the models, and comparison of the various predictions with each other. H. W. Sandusky (NSWC/WO) unveiled the experimental data on the second day, and the remainder of the time was spent comparing model predictions with this data.

[Experiment by Sandusky et. al./NSWC]

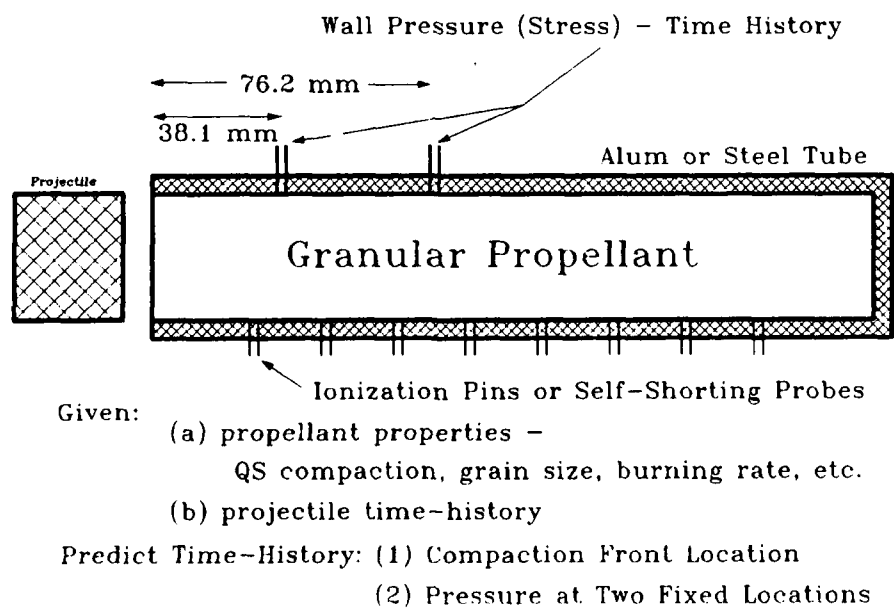


Fig. 1 - Schematic of Modeling Problem and NSWC Experiment [3].

II. PROBLEM DESCRIPTION

The modeling exercise, shown schematically in Fig. 1, is to simulate Sandusky's Piston-Driven-Compaction (PDC) experiment in which a quiescent granular sample is confined in an aluminum or heavy-wall steel tube (25.4 mm ID), and then subjected to impact by a cylindrical blunt-face Lexan projectile (300 mm long by 25.4 mm in diameter). Diagnostics include:

- (a) ionization pins and/or self-shorting probes at uniform intervals along the length of the tube,
- (b) microwave interferometry through the downstream end of the tube (looking toward the impacted end), and
- (c) flush-mounted pressure transducers in the tube wall at 38.1 mm and 76.2 mm from the impacted end.

The combination of (a) and (b) serves to locate the leading compaction front as a function of time. Further, the location of the projectile face after impact can be determined by the position of scribe lines on the cylindrical projectile photographed through a slit in the tube wall near the impacted end; this provides the time-dependent boundary condition for the modelers. More detail about this series of experiments can be found in Sandusky et. al. [3]. As the basis for this workshop, there were four PDC runs involving two different ball propellants. Two primary reasons motivated the selection of these materials; (1) compaction of an aggregate involves plastic deformation of grains [4], but not fracture [5], and (2) they are nearly spherical particles which might be expected to form a regular lattice which may be amenable to analysis [6]. Properties of both propellants are listed in Table I.

TABLE I. - PROPELLANT PROPERTIES

<u>Propellant Name</u>	WC-140	TS-3659
<u>Composition:</u>		
NC (nitrogen content = 13.05%)	98.53%	76.98%
NG	0.00%	21.57%
Stabilizer/Additive	1.47%	--
Diphenylamine	--	1.14%
Dinitrotoluene	--	0.31%
<u>Theoretical Maximum Density (g/cc)</u>	1.65	1.64
<u>Heat of Explosion (cal/g, experimental)</u>	919	1104
<u>Nominal Particle Size (μm)</u>	411 (spheres & "jelly beans")	434 (spheres)

Information Supplied to Modelers

(A) From the PDC Experiment:

The initial conditions for the modeling exercises were taken directly from the NSWC experiments [3]. Listed in Table II below are values for tube length (L), initial density (%TMD_o), the projectile velocity (V_p) just before impact, and the initial particle velocity (u) and compaction wave speed (U) just after impact. Of course, the values of particle velocity (the velocity of the projectile face after impact) and compaction wave speed will not necessarily remain constant. However, the modeler was also given the location of the projectile as a function of time after impact which could be used as a "piston" boundary condition; this avoids all the uncertainties associated with a description of the actual impact event.

Sandusky's [7] original PDC experiment performed in a Lexan tube produced the correlation " $\tau^2 \Delta t = \text{constant}$ ", where τ is a measure of the stress in the compacted solid phase and Δt is the time interval after impact before the appearance of visible flame (usually in material adjacent to the projectile face). It was intended that this modeling exercise would provide values of Δt for each propellant, which the modelers could use to help calibrate parameters in their reaction models. Several PDC runs were made in a Lexan tube with TS-3659 propellant, but the camera records showed no evidence of visible light; other observations, however, clearly indicated that reaction was underway. This "negative" finding may have important implications concerning the extent and/or type of reaction which begins the event. As a substitute in the four modeling problems, Sandusky examined both gage records and estimated the time at which rapid pressurization occurred. These two points in the x-t plane were used to linearly extrapolate back to the location of the projectile face. The value of time at the intersection defined a " Δt ", the time interval before the onset of rapid pressurization (not the appearance of visible flame). The modelers were provided a value (in one case, a range of values) of " Δt " for each of the problems.

 TABLE II. - INITIAL CONDITIONS FOR PDC MODELING PROBLEMS

PROPELLANT: TS-3659

Problem (PDC name)	%TMD _o	L(mm)	Tube	V _p (m/s)	u(m/s)	U(m/s)
#1 PDC-80	60.2	101.7	Alum	160	127	494
#2 PDC-81	60.1	146.8	Steel	237	192	534
#3 PDC-82	60.1	146.8	Steel	300	216	557

PROPELLANT: WC-140

#4 PDC-M30	60.5	146.8	Steel	210	161	563
------------	------	-------	-------	-----	-----	-----

(B) Quasi-Static Compaction Data:

Current models of compacted granular material are not yet capable of predicting the state of stress (including porosity) in the compressed aggregate. All of the theories involve parameters which must be calibrated by matching experimental data. For this purpose, quasi-static compaction experiments were performed over a range of mixture densities on both ball propellants using the double-piston in cylinder apparatus discussed in Campbell, Elban and Coyne [8]. Data supplied to the modelers included axial stress, radial stress, force applied to the driving ram, force transmitted to the passive ram, and the length of the sample volume. Differences between applied and transmitted force (along with the length measurement) allowed computation of the wall friction force. Determination of porosity required the modeler to estimate the compressibility of the solid material. For more detail on the experiment, see Sandusky et. al. [3].

(C) Propellant Ignition and Burning Rate Data:

A reasonable description of the burning rate of single-base WC-140 propellant over the pressure range 100 psi - 25 Kpsi was provided by a combination of recent strand burner data obtained by Price and Atwood [9] supplemented with BRL [10] closed-bomb data. Reference [9] also made available some recent ignition data generated from both arc image and CO₂ laser sources. For the double-base propellant TS-3659, burning rate information was incomplete. Strand burner data were nonexistent. This exercise relied entirely on NWC/China Lake closed-bomb data [11]. However, as is typical of the closed bomb, rates below approximately 2-3 Kpsi show the anomolous "tail off". Without low pressure strand data, the modelers were left to guess the rates at lower pressure, using the behavior of WC-140 as a guide. At the moment, there are no estimates of how sensitive the wave acceleration process is to variations in low pressure burning rate.

(D) Compressibility of TMD Propellant:

Although Hugoniot curves have been determined for many inert and explosive compounds, no information could be found for either WC-140 or TS-3659 propellant. As a substitute, some Russian data [12] for N-powder with a composition of approximately 40% NG in NC was provided, viz.,

$$V_s \text{ (km/s)} = 1.7 + 1.85 * u_s \text{ (km/s)}.$$

With 40% NG, this material will be slightly softer than either WC-140 or TS-3659, but the influence on the present modeling computations should be minimal.

Given this information, the modeler was asked in each case to provide predictions for (1) compaction wave locus, and (2) the time-history of whatever stress component a wall-mounted transducer should respond to at both gage locations. Because of complications involved with wave reflection from an end plug which was not well characterized, it was agreed that the computational problem will terminate when the leading compaction front strikes the downstream boundary (the far end of the PDC tube).

III. DISCUSSION OF RESULTS

Although the five models employed here were designed to solve a similar problem, there are many important differences which lead to a diversity of predictions. Unfortunately, the space limitations of this workshop summary will not permit a detailed discussion of the assumptions, mathematical formulation, and numerical solution techniques in each model. To help orient the reader, the Appendix contains a schematic overview of important aspects of each model. These schematics are not intended as a complete picture of the model; the cited references should be consulted for further detail, or questions should be addressed to the individual modeler in cases where documentation is not yet available. In the figures below which show comparison of model predictions to the experimental data of Sandusky et. al. [3], not all of the models are represented on each figure. This occurs because not all of the modelers brought predictions for all four exercises. Table III below can be used as a guide.

 TABLE III. - SUMMARY OF CONTRIBUTIONS

JANNAF PSHS WORKSHOP

"Model Predictions of the PDC Experiment"

25-26 October 1988, NASA/MSFC, Huntsville, AL

PREDICTIONS FOR → CONTRIBUTOR ↓	PDC-80 #1	PDC-81 #2	PDC-82 #3	PDC-M30 #4
Baer / SNLA	Yes	Yes	Yes	Yes
Kim & Hsieh/NSWC		Yes	Yes	
Kooker / BRL	Yes	Yes	Yes	Yes
Price / NWC	Yes	Yes	Yes	Yes
Weston / LLNL				Yes

Figures 2 through 9 show the comparison of modeling predictions with the experimental data. The figures are arranged in pairs; Fig. 2 is the compaction wave locus and Fig. 3 contains the two transducer time-histories for PDC-80 (Problem #1). Figures 4 and 5 pertain to PDC-81 (Problem #2), etc. In each figure, the top portion (a) is only the experimental data, and the bottom portion (b) shows the comparison of the model predictions with that data. Many of the comparison figures [(b) portion] are busy and somewhat confusing. A vertical line with the notation "end of problem" appears on each figure, and denotes the value of time at which the experimental data indicate the leading compaction front arrived at the end of the PDC tube. Beyond this value of time, the computational problem is over.

The nature of this problem is deceptive. The initial impact generates a strong compaction wave which propagates into the quiescent bed. Taking a simplistic view, not much happens behind this wave for a certain time interval; then suddenly the pressure can rise dramatically. The deception is in the region behind the compaction front where the pressure transducers may indicate that not much is happening. In fact there is apparently an intense competition between sources of heat generation (reactions) and heat loss mechanisms. The outcome of the competition produces the "timing" of a runaway (if one occurs). On the basis of the modeling predictions, a small change in a reaction parameter can lead to a major change in the timing of the runaway. Probably as no surprise, none of the models got everything "correct". A major conclusion from the Oct 1986 Workshop [2] is reinforced by the results from the present comparisons; compaction wave speed (and hence location) is a forgiving parameter. A close match of compaction wave locus does not necessarily mean a close match with the pressure transducers.

PDC-80 (Problem #1)

PDC-80, based on TS-3659 propellant, was run in the short tube (101.7 mm) and had the slowest initial projectile speed (160 m/s). As shown in Fig. 2a, the compaction wave locus is determined by two points dictated by the reporting time from each pressure transducer; PDC-80 was the only run which did not have microwave interferometry. As shown in Fig. 2b, all three predictions are close to the first data point, with some divergence toward the latter stages of propagation. The sudden "turn up" predicted by Baer (SNLA) cannot be confirmed with the two data points available. The "slow down" predicted by Price (NWC) may be partly the result of his time-dependent boundary condition. In all his computations, Price (NWC) elected to use a lumped-mass solution of projectile impact on the granular bed, rather than employ the given experimental projectile location as a function of time as a "piston" boundary condition. This solution predicted a time-dependent location of the projectile face which differed from the experimental observation.

The time-history from both pressure transducers is shown in Fig. 3a. Both gages confirm the onset of rapid pressurization, although the rapid rise of gage #2 occurs beyond the time ($\sim 204 \mu\text{s}$) at which the leading compaction front reached the end of the PDC tube. There are two common features in the gage responses from all four PDC runs. The first one is clearly evident here in the record from Gage #2, and to a lesser extent from Gage #1. This is the almost linear "decay" of the report value after the gage has been uncovered, before the beginning of rapid pressurization presumably due to significant reaction [see Fig. 10 also]. None of the models predicted this behavior. There was considerable discussion about the possible physics involved, as well as the possibility of gage anomalies. One suggestion was rate-dependent stress behavior in the suddenly compacted aggregate, which might influence the deviator stress component and hence play a role in the stress value which is being measured by the wall-mounted transducer. The issue was not resolved. The second feature is the smaller magnitude of initial response (and subsequent values before reaction begins) reported by Gage #2 compared to Gage #1. This is most likely the influence of wall boundary friction. Of the three model calculations illustrated in Fig. 3b, Price's (NWC) model was the only one to account for wall friction and it predicts this effect. Figure 3a also illustrates another trend when comparing model predictions with the transducer records. Both Kooker (BRL) and Baer (SNLA) predict an initial level of gage response which exceeds the experimental

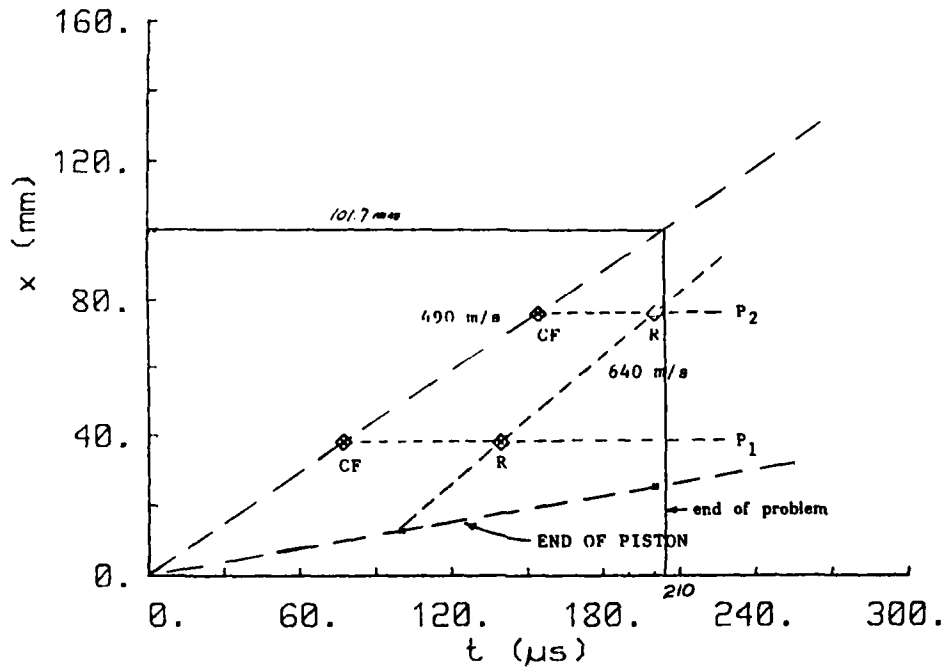


Fig. 2a - Compaction Wave Locus for PDC-80 (Problem #1); 160 m/s Impact on 60.2% TMD TS-3659. Tube Length is 101.7 mm. Experimental Data from Sandusky et. al. [3].

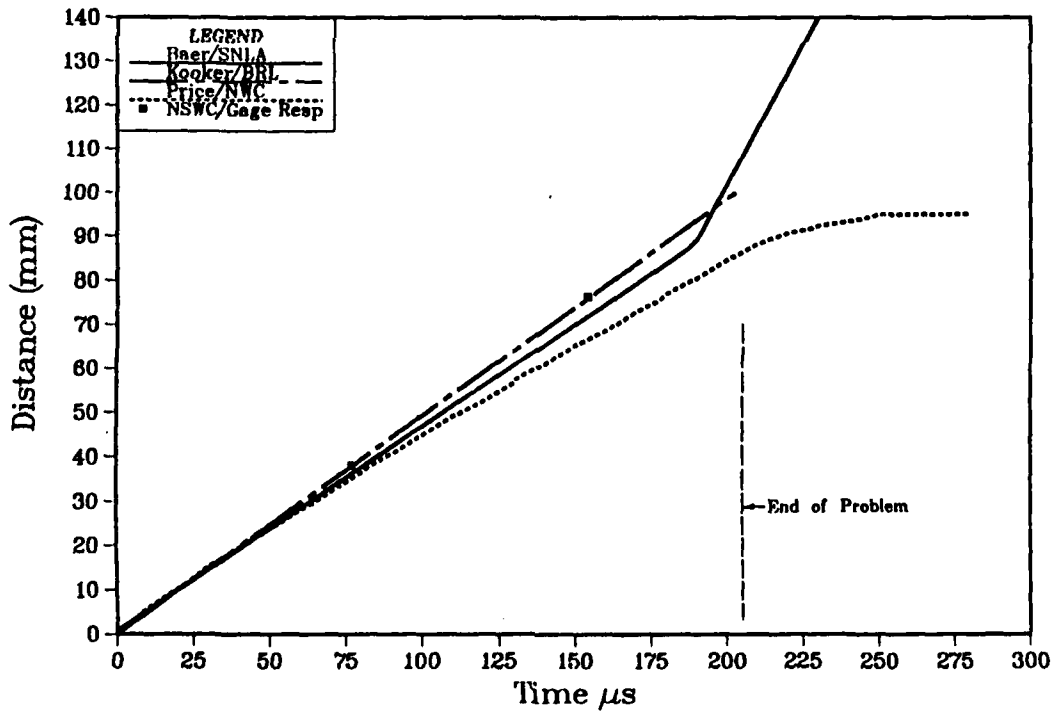


Fig. 2b - Compaction Wave Locus for PDC-80 (Problem #1); 160 m/s Impact on 60.2% TMD TS-3659. Comparison of Workshop Predictions with Data from Sandusky et. al. [3].

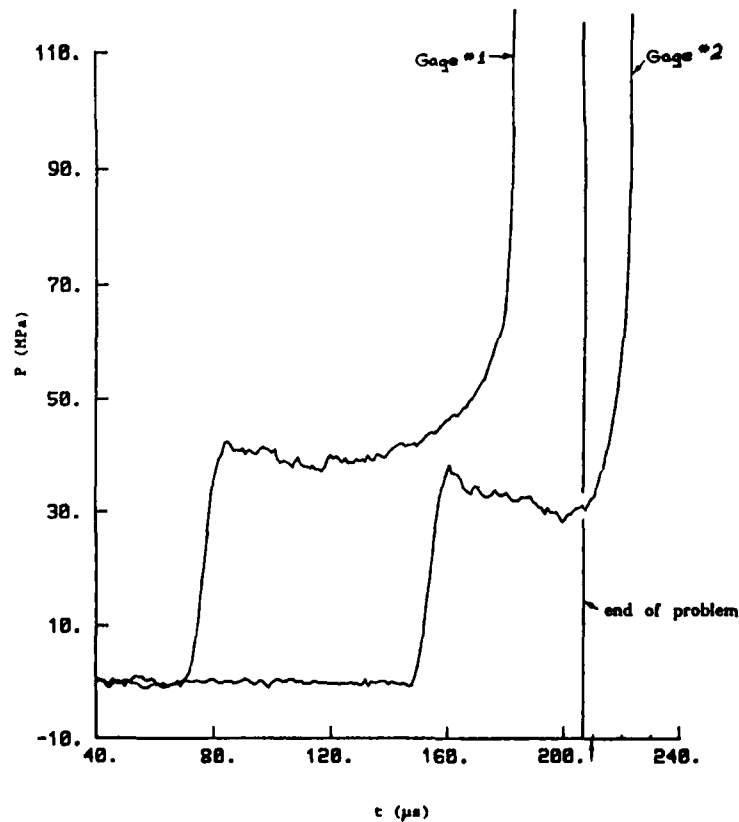


Fig. 3a - Time-History From Wall-Mounted Transducers for PDC-80 (Problem #1); 160 m/s Impact on 60.2% TMD TS-3659. Experimental Data from Sandusky et. al. [3]. Gage #1 is Located at 38.1 mm, and Gage #2 at 76.2 mm; Tube Length is 101.7 mm.

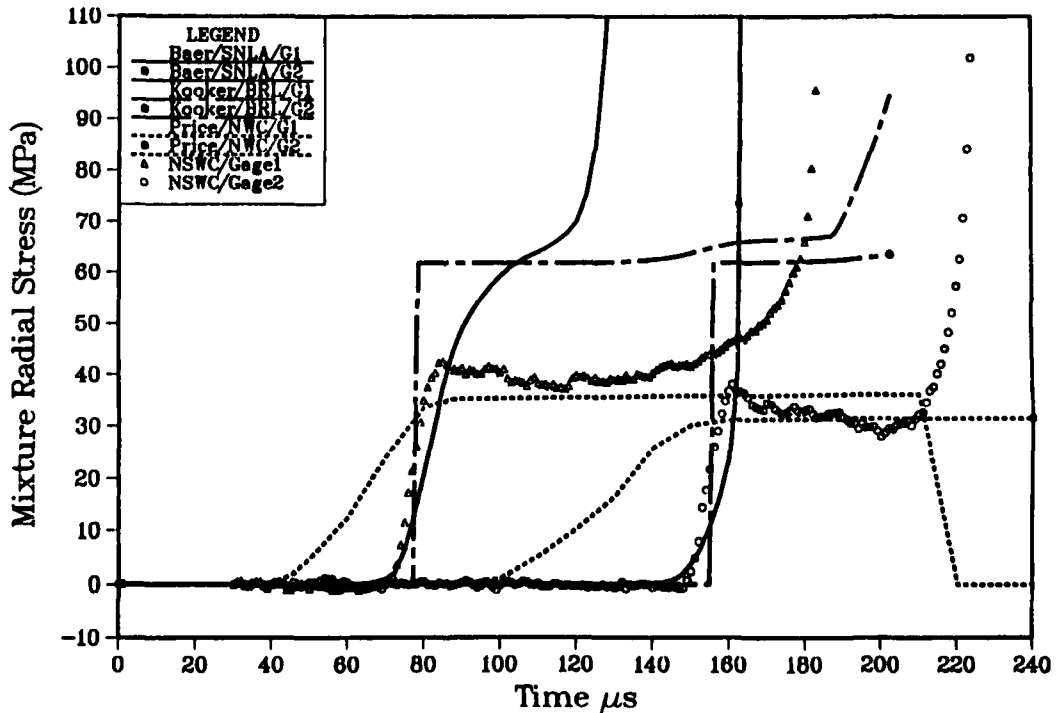


Fig. 3b - Time-History From Wall-Mounted Transducers for PDC-80 (Problem #1); 160 m/s Impact on 60.2% TMD TS-3659. Comparison of Workshop Predictions with Data from Sandusky et. al. [3]. Gage #1 is Located at 38.1 mm, and Gage #2 at 76.2 mm; Tube Length is 101.7 mm.

value. The mathematical formulation in all three models (at the time of the Workshop) treated the stress tensor of the compressed aggregate as a pressure, and ignored deviator components. Both Kooker (BRL) and Baer (SNLA) based their predictions for gage response on this value of mixture pressure. However, the quasi-static compaction data [3] for TS-3659 distinctly shows the presence of a deviator component which leads to a significant reduction in the value of radial stress. The data [3] indicate that the ratio of the radial stress component to the axial component varies with the state of compaction. Price (NWC) chose an average value of 0.6 as representative of the data, and multiplied his predictions for pressure by this value to get gage response. As the comparison in Fig. 3b indicates, these values are more realistic. The important implication is that the dynamically-formed aggregate in both materials apparently supports deviator stress components which are similar to the quasi-static stress state. The wall-mounted transducers are responding to the radial component.

Compaction wave thickness can also be estimated from the transducer records, assuming wave speed is known. For example, Gage #1 in Fig. 3 indicates a rise time of approximately 12 μ s which implies a wave thickness of 6 mm if the speed is taken as 0.5 mm/ μ s. Recall that Sandusky's [7] earlier work utilizing flash radiography in a Lexan tube estimated the wave thickness as the distance between two tracer wires, i.e., 6.35 mm. Model predictions of wave thickness (or gage rise time) are significantly influenced by the equation formulation and the numerical solution technique. If the equation system neglects the diffusive effects of Fourier heat conduction (not heat transfer between phases), viscous stresses (not the drag force between phases), and rate-dependent resistance forces during porosity adjustments in the aggregate (often modeled with a "compaction viscosity"), then the mathematical solution for a compaction wave is a shock wave with zero thickness. If the numerical solution predicts otherwise, the finite thickness is due to artificial diffusion added by the numerical integration technique. Baer's (SNLA) formulation, which does account for rate-dependent porosity adjustments and hence includes a physical basis for a finite thickness wave, predicts a gage rise behavior quite similar to the experimental data. This is a definite achievement. Kooker (BRL) assumes instantaneous adjustment (zero compaction viscosity) to the equilibrium stress state and then tracks compaction waves as infinitesimally-thin shock waves with the method-of-characteristics; the predictions show a zero-thickness wave which passes the gage location near the mid-point of the rise time. Price's (NWC) formulation also neglects rate-dependent resistance (other than inertial forces) to porosity change, but the solution predicts a wave thickness somewhat greater than the data.

Both gage records in Fig. 3 confirm that some type of reaction process was under way near the end of this PDC experiment. The comparisons in Fig. 3b also testify to the difficulty the models had in predicting the timing of this pressure rise. The input data supplied to the modelers was insufficient to calibrate all the "reaction parameters" in the various formulations. The remaining values had to be "guessed", or estimated by comparison to other available data on similar materials. Unfortunately, a slight variation in some of these values could often mean the difference between benign behavior and a runaway. As seen in Fig. 3b, Baer's (SNLA) computations show a premature runaway, Kooker's (BRL) computations show a turn-up closer to the gage records (probably fortuitous), and Price's (NWC) computations indicate no runaway.

PDC-81 (Problem #2)

PDC-81 is also based on TS-3659 propellant, but was run in the 146.8 mm long heavy-wall steel tube using a higher initial projectile speed of 237 m/s. The leading compaction front locus, as shown in Fig. 4a, is defined in detail by the data from the microwave interferometer. Compaction wave speed is virtually constant at 534 m/s until late in the run when it abruptly increases to 1800 m/s. Comparing model predictions to this data in Fig. 4b shows that all four calculations are close to the experiment until approximately half way down the tube. Baer's (SNLA) model prematurely predicts an abrupt increase in speed, but the new velocity is nearly equal to what the experiment will eventually do. This is encouraging. Again, timing of the event can be difficult to predict. Kim and Hsieh's (NSWC) model predicts a violent runaway event with the wave about midway down the tube, and this halts the calculation (see the predicted pressure history in Fig. 5b). Kooker's (BRL) model predicts a mild turn-up just as the wave approaches the end of the tube, and Price's (NWC) model does not yet show the effects of reaction.

The model predictions for wall stress time-history are compared to the transducer records in Fig. 5. For each of the four models, the predicted behavior of the compaction front locus discussed above is mirrored in their stress predictions. Although the overall slopes of a couple of the runaway curves are similar to the data, the predicted timing of the event is poor. Some discussion in the workshop arose over the "plateau" behavior (near 200 MPa) of the Gage #1 response between 180-210 μ s. The question was what mechanism is responsible for the 20-30 μ s "pause" in the growth of pressure? One speculation was an anomaly in "hot spot" compressive combustion. Another speculation was the influence of expansion waves generated by a slow down (or reversal of direction?) of the projectile, i.e., a loss of confinement. This second speculation highlights a nagging problem in these exercises. Because of experimental difficulties, the position of the projectile, after impact, is sometimes known only during the early time of the experiment (in PDC-81, only up to 92 μ s). Furthermore, in those runs based on higher projectile impact speeds, there is little doubt that the Lexan projectile deforms; Sandusky attempts to account for this deformation when interpreting the position of the scribe lines on the body of the projectile. Thus, (a) the modeler may not have the complete time-dependent boundary condition, and (b) its accuracy is in question. Sandusky suggested that any future experiments of this type should be run with an aluminum projectile.

PDC-82 (Problem #3)

PDC-82 is still based on TS-3659 propellant confined in the 146.8 mm long heavy-wall steel tube, but involved a 300 m/s impact. This was a more energetic event which produced an increase in speed to 2110 m/s as shown in Fig. 6 by the compaction front locus defined by the microwave interferometry. The model predictions for compaction front locus are fairly close to the data until the vicinity of the turn. The two closest predictions were Price's (NWC) model which turned up early and Baer's (SNLA) model which was slightly late, but both suggested a speed in the correct range. Kim and Hsieh's (NSWC) model did not show a significant change in wave speed, but the pressure field is increasing dramatically at the end of the computation. Kooker's (BRL) model ran into numerical difficulties in attempting the turn, which terminated the calculation. (text continues on page 26).

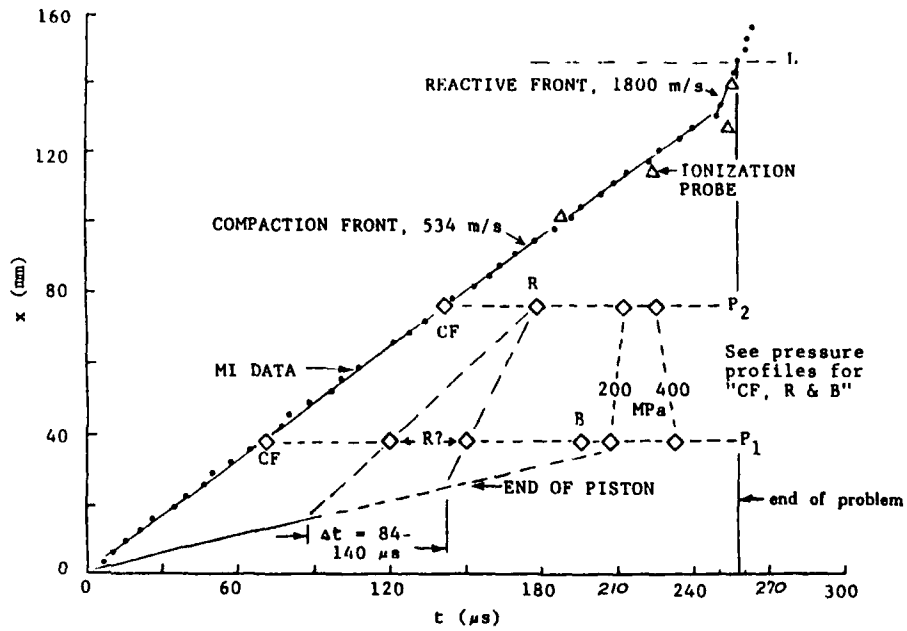


Fig. 4a - Compaction Wave Locus for PDC-81 (Problem #2); 237 m/s Impact on 60.1% TMD TS-3659. Tube Length is 146.8 mm. Experimental Data of Sandusky et. al. [3].

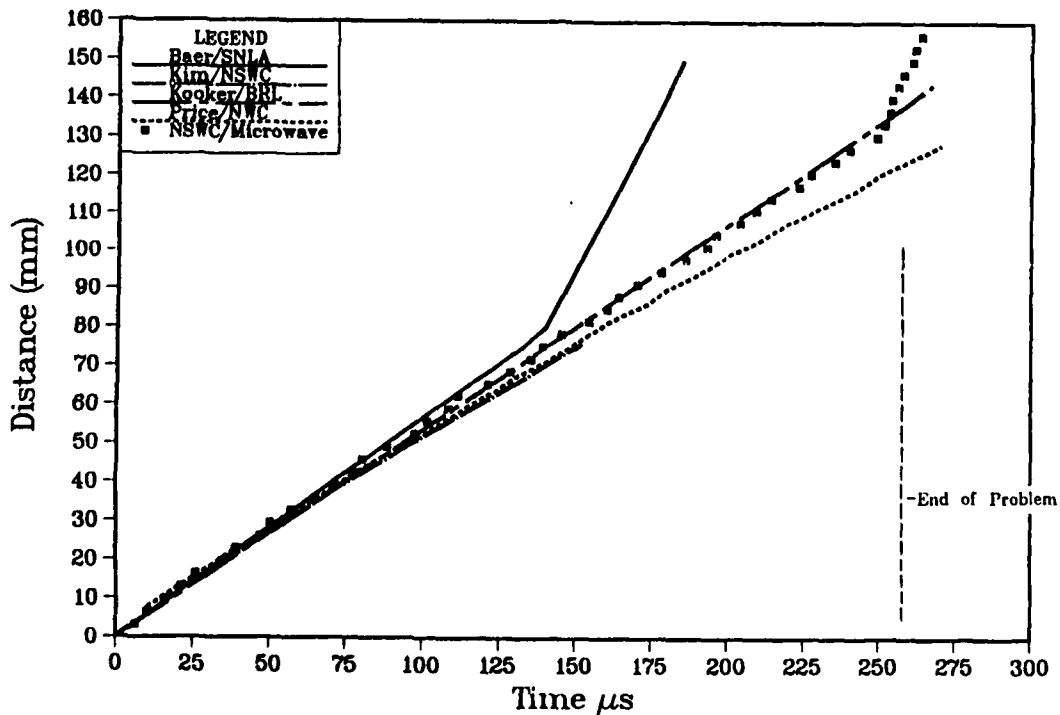


Fig. 4b - Compaction Wave Locus for PDC-81 (Problem #2); 237 m/s Impact on 60.1% TMD TS-3659. Comparison of Workshop Predictions with Microwave Data from Sandusky et. al. [3].

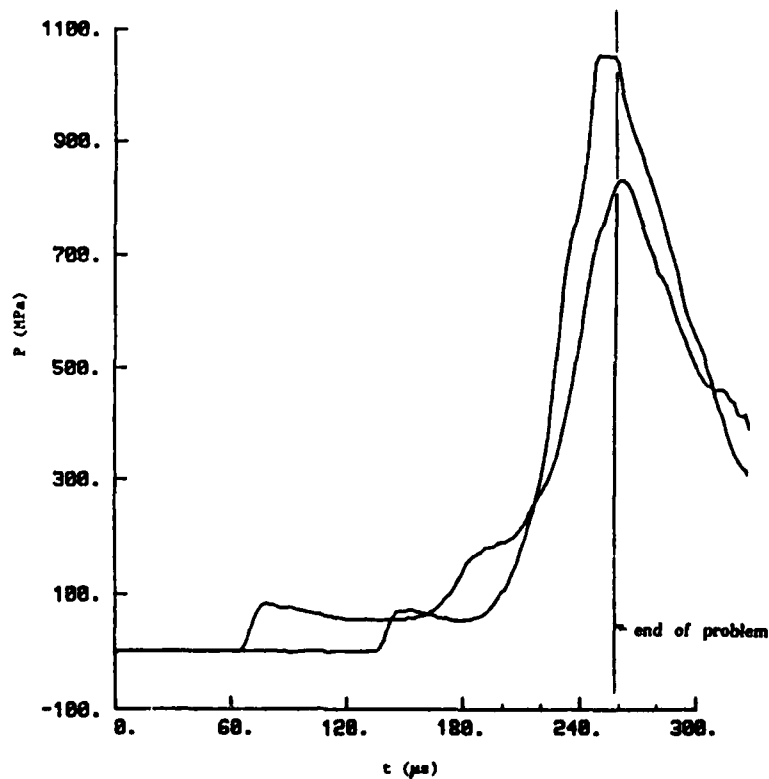


Fig. 5a - Time-History From Wall-Mounted Transducers for PDC-81 (Problem #2); 237 m/s Impact on 60.1% TMD TS-3659. Experimental Data from Sandusky et. al. [3]. Gage #1 is Located at 38.1 mm, and Gage #2 at 76.2 mm; Tube Length is 146.8 mm.

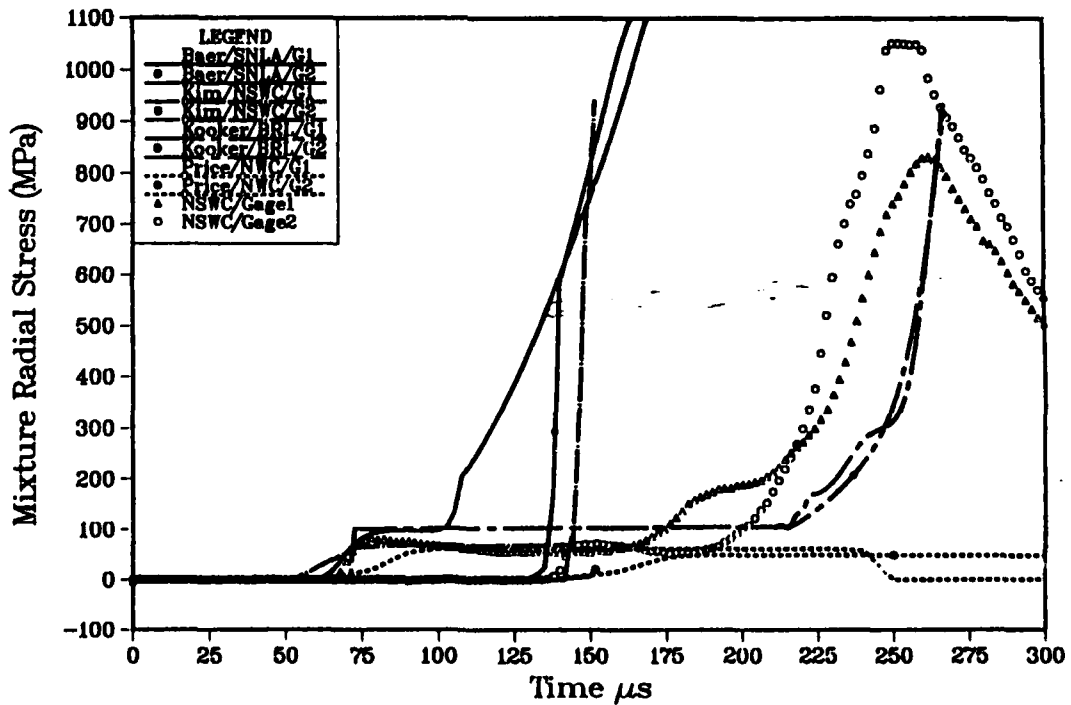


Fig 5b - Time-History From Wall-Mounted Transducers for PDC-81 (Problem #2); 237 m/s Impact on 60.1% TMD TS-3659. Comparison of Workshop Predictions with Data from Sandusky et. al. [3]. Gage #1 is Located at 38.1 mm, and Gage #2 at 76.2 mm; Tube Length is 146.8 mm.

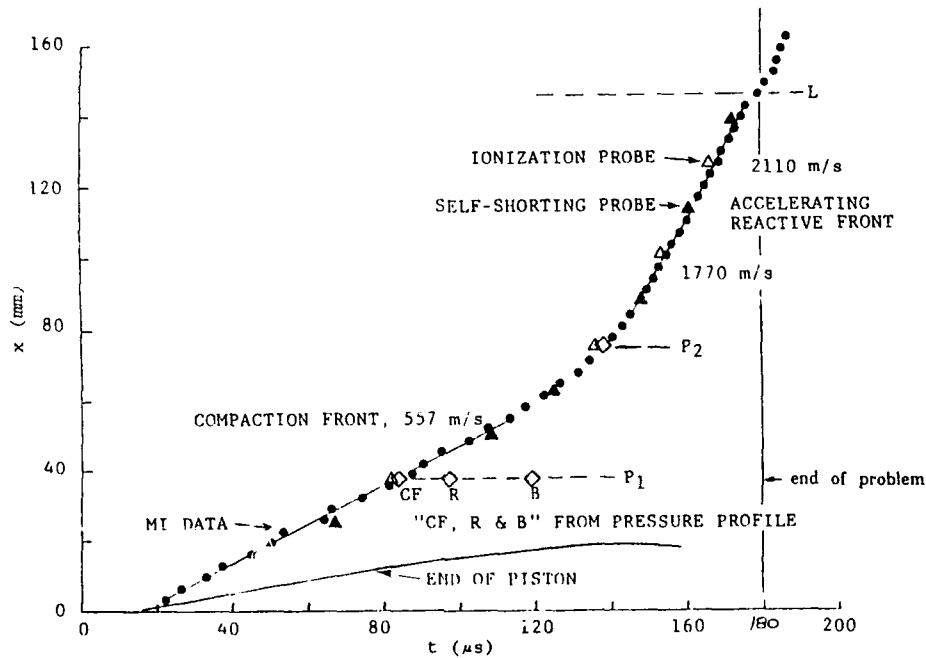


Fig. 6a - Compaction Wave Locus for PDC-82 (Problem #3); 300 m/s Impact on 60.1% TMD TS-3659. Tube Length is 146.8 mm. Experimental Data of Sandusky et. al. [3].

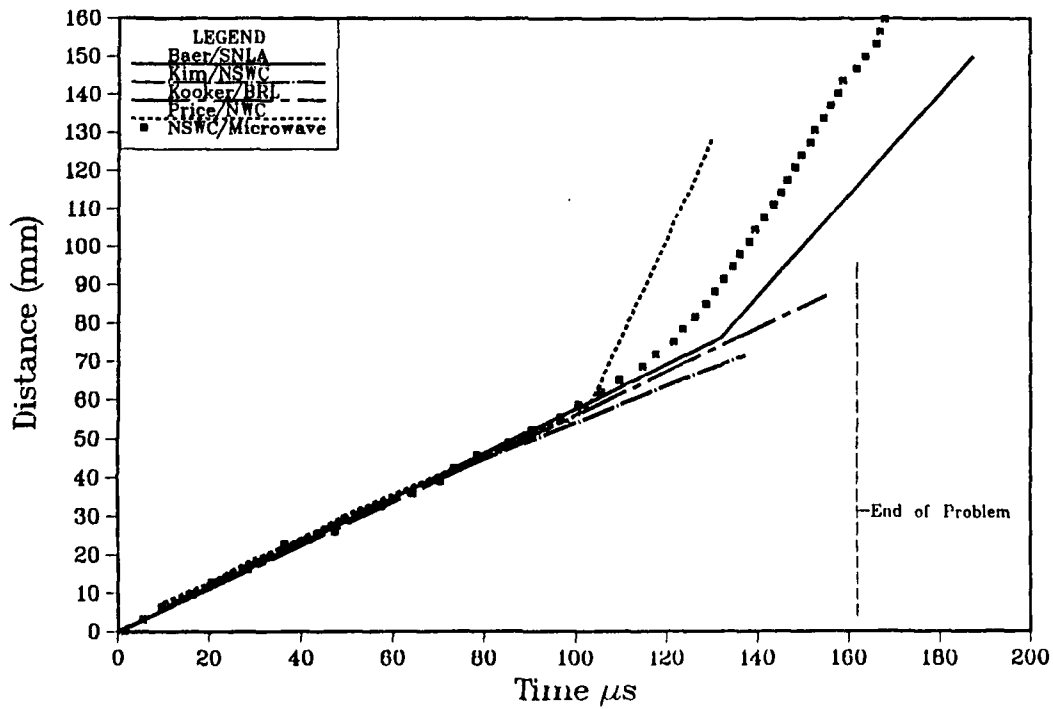


Fig. 6b - Compaction Wave Locus for PDC-82 (Problem #3); 300 m/s Impact on 60.1% TMD TS-3659. Comparison of Workshop Predictions with Microwave Data from Sandusky et. al. [3].

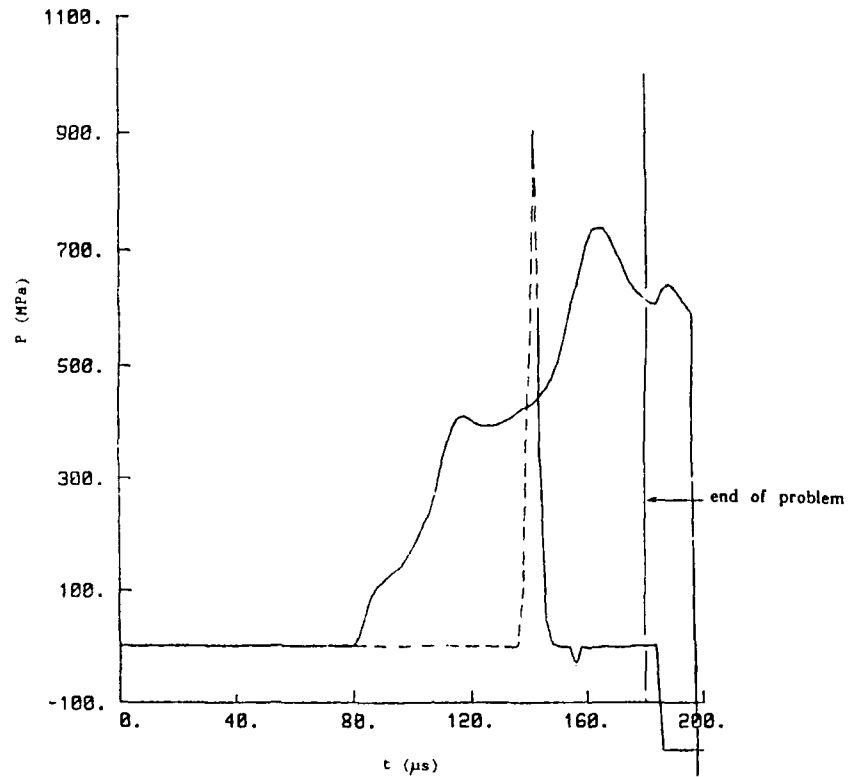


Fig. 7a - Time-History From Wall-Mounted Transducers for PDC-82 (Problem #3); 300 m/s Impact on 60.1% TMD TS-3659. Experimental Data from Sandusky et. al. [3]. Gage #1 is Located at 38.1 mm, and Gage #2 at 76.2 mm; Tube Length is 146.8 mm.

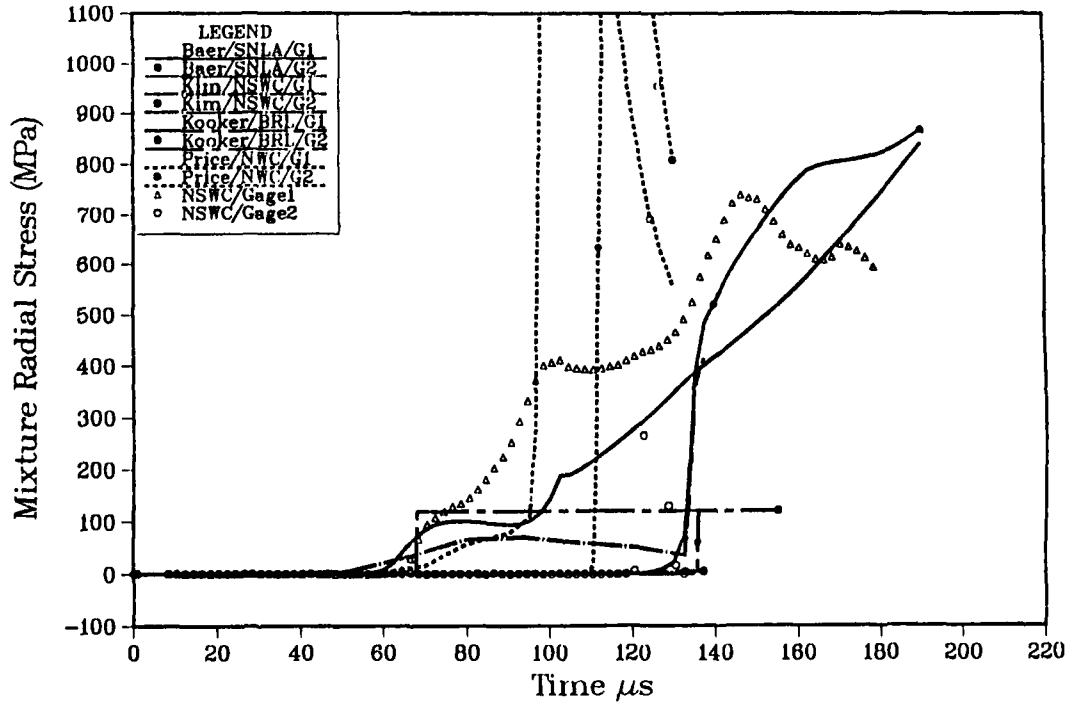


Fig. 7b - Time-History From Wall-Mounted Transducers for PDC-82 (Problem #3); 300 m/s Impact on 60.1% TMD TS-3659. Comparison of Workshop Predictions with Data from Sandusky et. al. [3]. Gage #1 is Located at 38.1 mm, and Gage #2 at 76.2 mm; Tube Length is 146.8 mm.

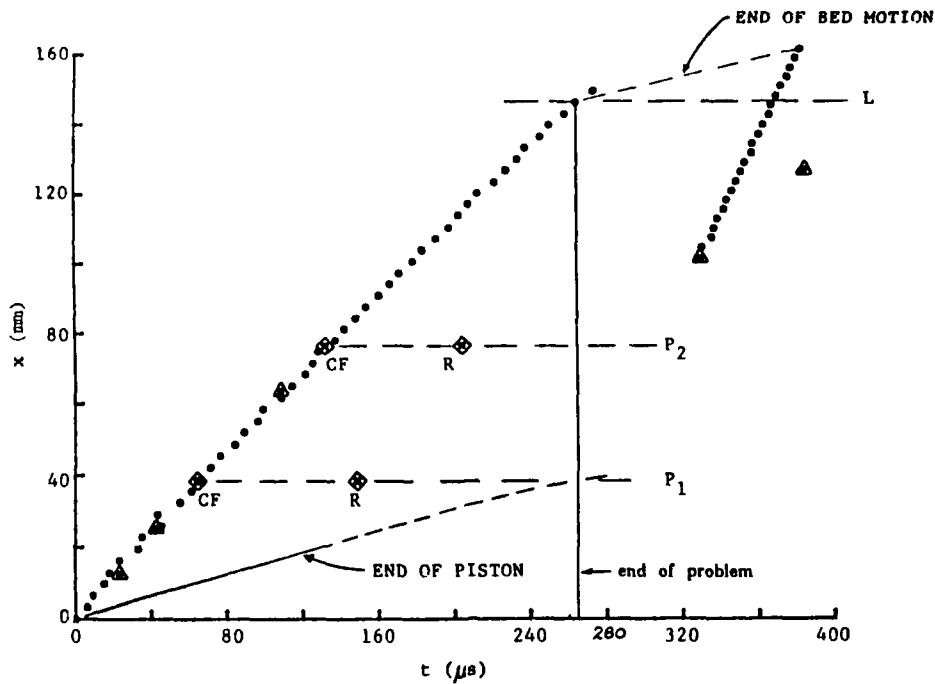


Fig. 8a - Compaction Wave Locus for PDC-M30 (Problem. #4); 210 m/s Impact on 60.5% TMD WC-140. Tube Length is 146.8 mm. Experimental Data from Sandusky et. al. [3].

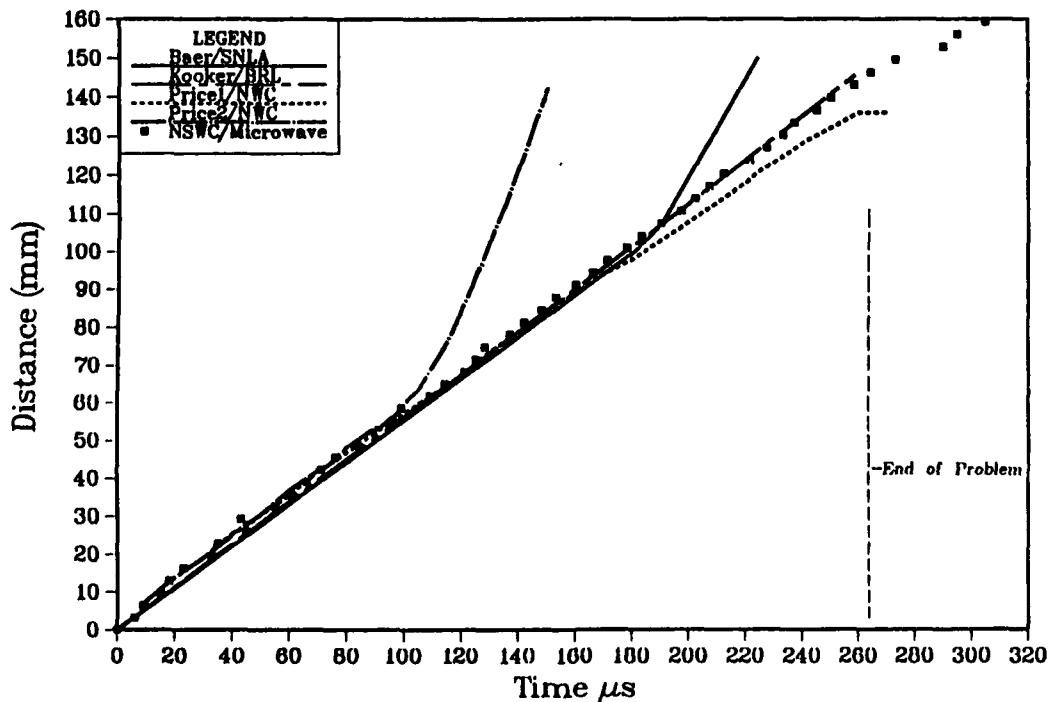


Fig. 8b - Compaction Wave Locus for PDC-M30 (Problem #4); 210 m/s Impact on 60.5% TMD WC-140. Comparison of Workshop Predictions with Microwave Data from Sandusky et. al. [3].

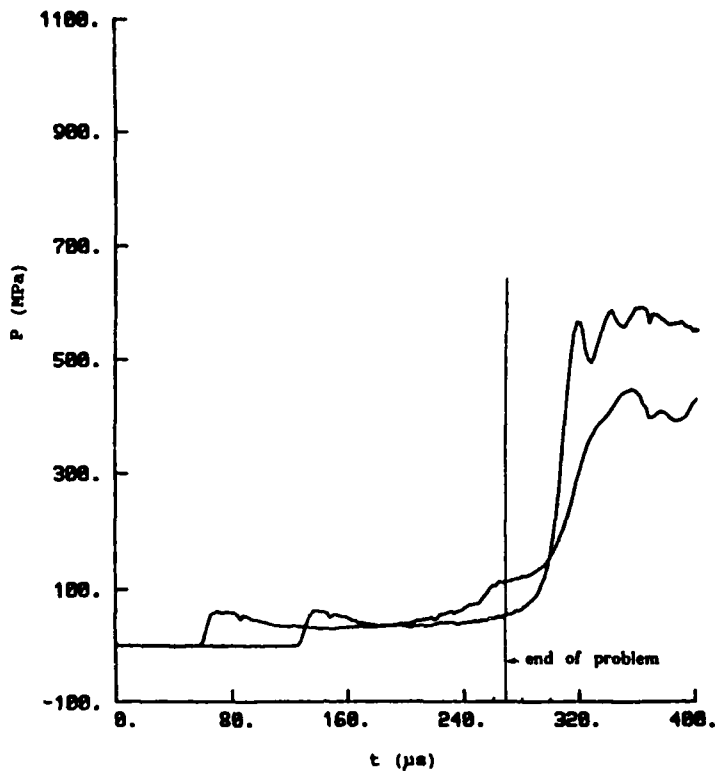


Fig. 9a - Time-History From Wall-Mounted Transducers for PDC-M30 (Problem #4); 210 m/s Impact on 60.5% TMD WC-140. Experimental Data from Sandusky et. al. [3]. Gage #1 is Located at 38.1 mm, and Gage #2 at 76.2 mm; Tube Length is 146.8 mm.

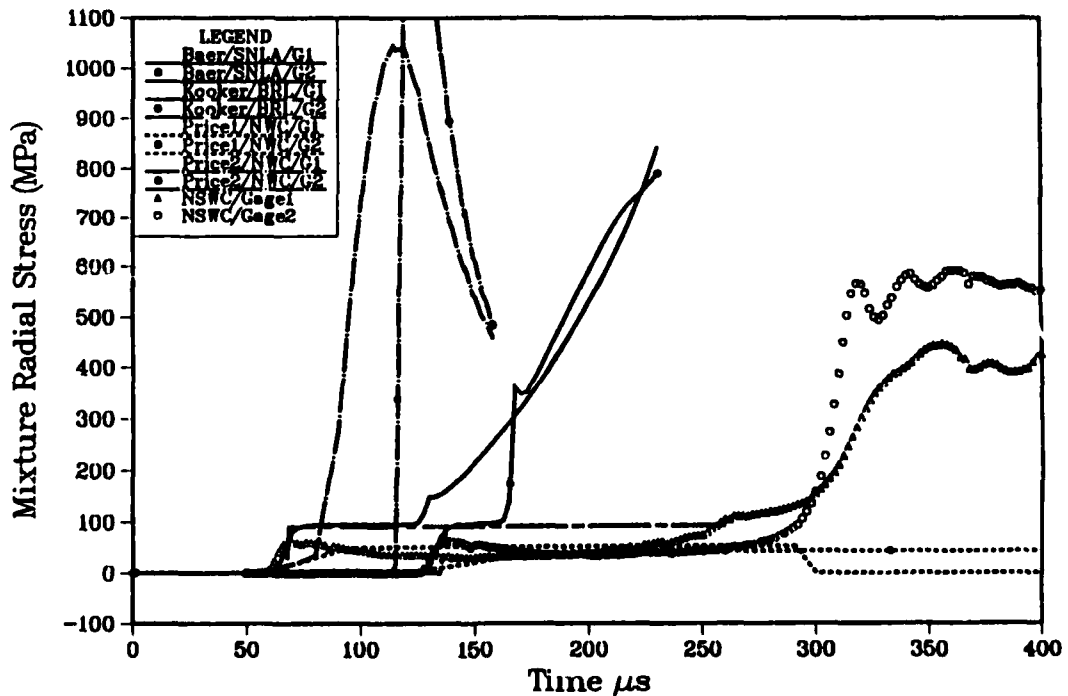


Fig. 9b - Time-History From Wall-Mounted Transducers for PDC-M30 (Problem #4); 210 m/s Impact on 60.5% TMD WC-140. Comparison of Workshop Predictions with Data from Sandusky et. al. [3]. Gage #1 is Located at 38.1 mm, and Gage #2 at 76.2 mm; Tube Length is 146.8 mm.

The transducer records from PDC-82 shown in Fig. 7 confirm the strength of the combustion event. Gage #2 sees a strong shock-like wave, while Gage #1 displays some unusual undulations. None of the models came very close to these records. Possibly projectile motion after impact has led to a complicated system of expansion waves which influence the response at Gage #1; Sandusky (NSWC) commented that the reaction in this run was violent enough to virtually force the projectile back out of the tube.

PDC-M30 (Problem #4)

PDC-M30 changed propellant to the less energetic single-base WC-140, but was conducted in the 146.8 mm long heavy-wall steel tube. Projectile impact speed was 210 m/s. Compaction front locus is displayed in Fig. 8, which shows an unusual behavior after approximately 270 μ s as the compacted bed forces the end plug out of the tube. The microwave interferometry has tracked the motion of a second wave front (apparently driven by combustion) in the bed as it is being expelled. As a conciliatory gesture, the modelers were not held accountable for this late time behavior. Up to 270 μ s, the compaction front moves at nearly constant speed, which most of the models predicted until the onset of significant reaction. Price (NWC) offered two predictions which differed only by a slight change in one of his reaction parameters; the influence on the predicted wave locus was substantial.

The transducer time-histories are compared to the model predictions in Fig. 9. Unfortunately, the significant rise seen by both gages occurred after 270 μ s when the compaction front reached the downstream end of the tube. Baer (SNLA) and Kooker (BRL) were close to the reporting time of the gages, while Price's (NWC) "number 1" prediction gives a better representation of the low magnitudes from both transducers [see Fig. 10]. Weston's (LLNL) predictions are compared to the data separately in Fig. 11 and seem to show evidence of an instability (Weston discovered an error in his gas-phase equation-of-state after the Workshop). None of the predictions could be considered as accurate. Again, timing of the runaway pressure field is a delicate prediction.

IV. CONCLUDING REMARKS

During the course of the Workshop, a number of discussions arose about the behavior of the strong compaction wave and how the theories are modeling its role in initiating reaction. Apparently there are many cases where the experimental value of compaction wave speed exceeds the model prediction for an inert wave, when the model is based on rate-independent porosity change which is calibrated with the quasi-static compaction data. The question of what mechanism(s) is responsible for the increase in speed seems to have provoked two schools of thought. The first one suggests that a rate-dependent visco-plastic material response of the aggregate would produce a stiffer material and thus support a higher wave speed. This dynamic stress state would look nearly time-invariant to the PDC experiment if the aggregate's characteristic relaxation time is large enough. The question of how this behavior would influence the compaction wave thickness has not been answered. The question of how the reaction begins in the compressed aggregate still remains. The second school of thought is that these compaction fronts are not inert; the high strain rate in the wave front itself begins the reaction process. Of course, many new questions now arise concerning what type of reaction begins and how much energy is released. There is little consensus from this point on. There is also the

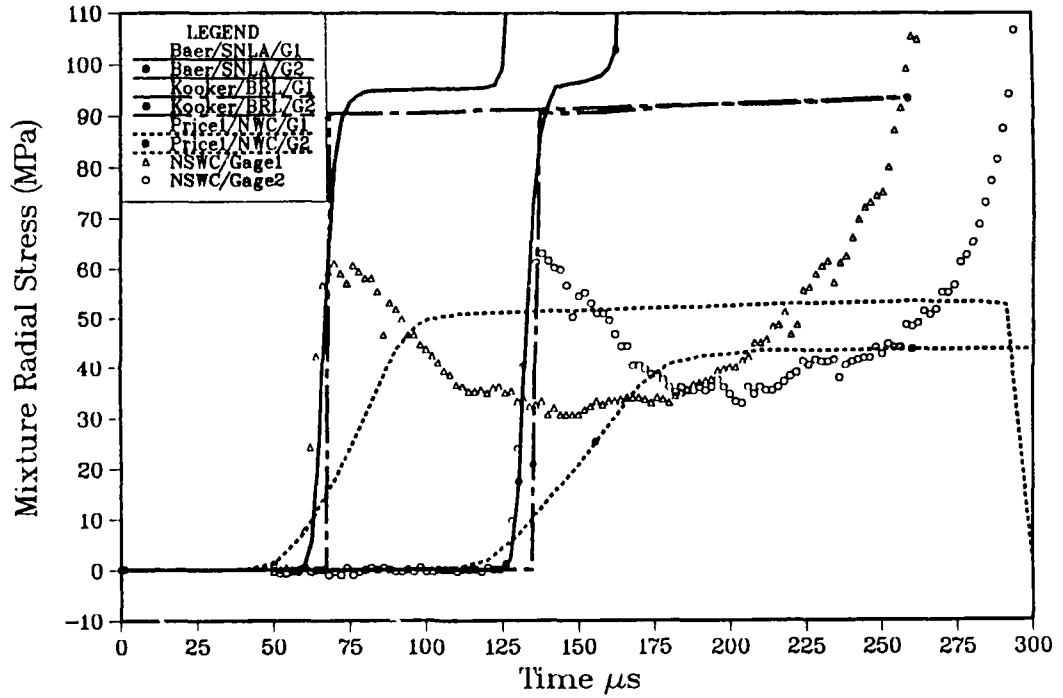


Fig. 10 - Time-History From Wall-Mounted Transducers for PDC-M30 (Problem #4); 210 m/s Impact on 60.5% TMD WC-140. Comparison of Workshop Predictions with Data from Sandusky et. al. [3]. Scale to Illustrate Low Level Gage Response.

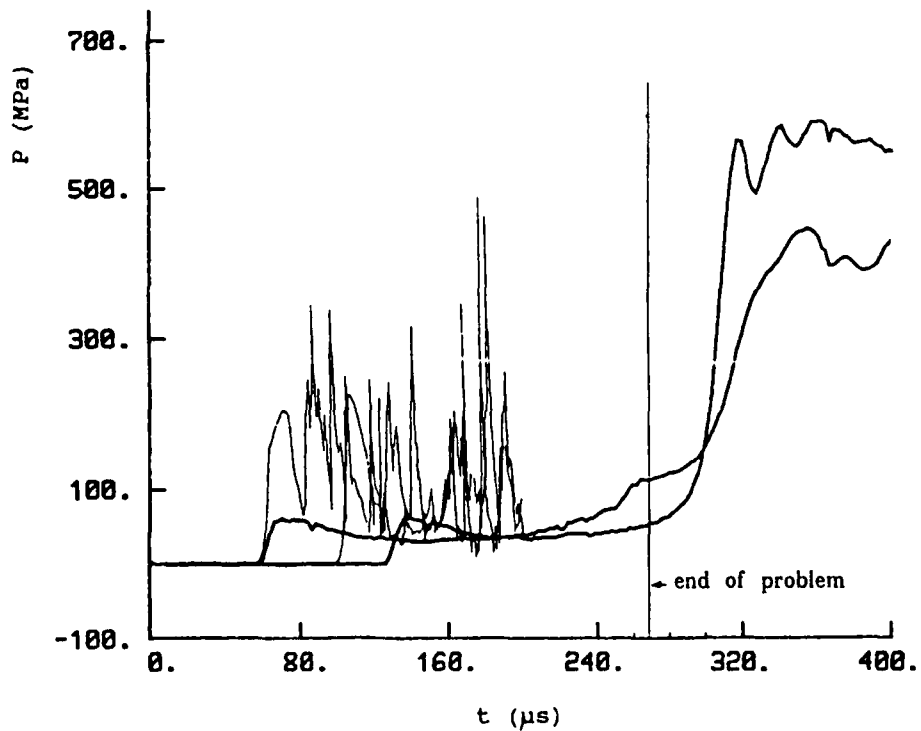


Fig. 11 - Time-History From Wall-Mounted Transducers for PDC-M30 (Problem #4); 210 m/s Impact on 60.5% TMD WC-140. Comparison of Workshop Predictions From Weston with Data from Sandusky et. al. [3]. Gage #1 is Located at 38.1 mm, and Gage #2 at 76.2 mm; Tube Length is 146.8 mm.

possibility that the real compaction wave is reactive and exhibits rate-dependent material behavior.

Since a number of the modelers are assuming that the compaction wave is not inert, there were additional discussions about what reaction is being modeled. There appear to be two broad categories here, (a) condensed-phase "hot spot" reactions, and (b) gas-phase reactions. Some models include both. There was no consensus on how to model hot spot reactions. A couple of the models which include gas-phase reactions assume that the reactants originate as products from the condensed-phase reactions. Postulating the existence of reactive gas-phase species leads to an interesting question about the extent of heat release in the condensed-phase reactions. The early PDC experiments on TS-3659 in a Lexan tube showed no indication of visible radiation, which would seem to constrain gas-phase temperatures well below an equilibrium flame temperature. Thus the sketchy evidence so far would suggest the initial gas-phase reactants, if they exist, are intermediate products which then could react further at some later time. Release of this final heat of combustion would be a contributor to ignition of the remaining portion of the compressed aggregate.

The results of the Workshop might be summarized with the following:

(1) The compaction front locus (position vs. time) and hence compaction wave speed are forgiving parameters. Agreement with this data does not guarantee that the model can predict the pressure transducer records.

(2) The impact-generated compaction wave apparently sets off an intense competition in the compressed aggregate between various reaction sources and heat loss; the outcome determines the time of a runaway pressure field. Current models have difficulty making this prediction. Besides the numerical solution complexities, the primary reason is uncertainty about the reaction sources, how to model these sources and then calibrate the inevitable unknown parameters.

(3) When comparing model predictions with the PDC experimental data:

(a) several of the models were able to predict the general wave mechanics (time at which each gage reports, wave thickness, etc.)

(b) the wall-mounted transducer data show an almost linear "decay" after the initial report value, until the onset of significant reaction. None of the models predict this, and it has not been explained.

(c) the initial value reported by the second transducer is less than that reported by the first transducer. Wall-boundary friction is the likely cause.

ACKNOWLEDGEMENTS

This Workshop would not have been possible without the creative ideas and hard work of Dr. Harold W. Sandusky of the Naval Surface Warfare Center / White Oak Laboratory. The chairman and all the participants extend their sincere appreciation. Several individuals deserve special recognition for their invaluable contributions to the success of these modeling exercises:

Quasi-Static Compaction Data -

Mr. Ralph L. Campbell of NSWC / WO
Prof. Wayne L. Elban and Prof. Paul J. Coyne, Jr., of Loyola College /
Baltimore, MD.

Ignition and Burning Rate Data -

Mr. Channon F. Price and Dr. Alice Atwood of NWC / China Lake.

PDC Experiments and Microwave Interferometry -

Dr. Harold W. Sandusky and Mr. Brian C. Glancy of NSWC / WO.

REFERENCES

1. D. E. Kooker and M. Costantino, "Mechanical Properties of Compacted Granular Material: A Workshop Summary", 1986 JANNAF Propulsion Systems Hazards Meeting, CPIA Publication 446, Vol. I, pp. 81-98, March 1986 [see also BRL TR-2835, September 1987, U. S. Army Ballistic Research Laboratory].
2. D. E. Kooker, "A Workshop Summary of Compaction Waves in Granular Material: Numerical Predictions", 1987 JANNAF Propulsion Systems Hazards Meeting, CPIA Publication 464, Vol. I, pp. 127-138, March 1987 [see also BRL TR-2836, September 1987, U. S. Army Ballistic Research Laboratory].
3. H. W. Sandusky, B. C. Glancy, R. L. Campbell, A. D. Krall, W. L. Elban and P. J. Coyne, Jr., "Compaction and Compressive Reaction Studies for a Spherical, Double-Base Ball Propellant", 25th JANNAF Combustion Meeting, 24-28 October 1988, NASA/Marshall Space Flight Center, Huntsville, AL.
4. W. L. Elban, "Quasi-Static Compaction Studies for DDT Investigations. Ball Propellants", **Propellants, Explosives & Pyrotechnics**, Vol. 9, pp. 119-129, 1984.
5. W. L. Elban and M. A. Chiarito, "Quasi-static Compaction Study of Coarse HMX Explosive", **Powder Technology**, Vol. 46, pp. 181-193, 1986.
6. S. J. Jacobs and H. W. Sandusky, "Modeling of Porous Bed Compaction with Deformed Spheres in a Regular Lattice", 1986 JANNAF Propulsion Systems Hazards Meeting, CPIA Publication 446, Vol. I, pp. 149-162, March 1986.
7. H. W. Sandusky and R. R. Bernecker, "Compressive Reaction in Porous Beds of Energetic Materials", **Eighth Symposium (International) on Detonation**, NSWC MP 86-194, pp. 881-891, July 1985.
8. R. L. Campbell, W. L. Elban and P. F. Coyne, Jr., "Side-Wall Pressure Measurements in Quasi-Static Compaction of Porous Beds of HMX Powders and ABL-2523 Casting Powders", 1988 JANNAF Propulsion Systems Hazards Meeting, 28-31 March 1988, The Aerospace Corp., Los Angeles, CA.
9. C. F. Price and A. Atwood, Naval Weapons Center, China Lake, CA, private communication of ignition and strand burner data for M10 propellant, 1988.
10. BRL closed bomb burning rates for M10 propellant, as reported in "Round Robin Results of the Closed Bomb and Strand Burner", CPIA Publication 361, p. I-15, July 1982.
11. NWC Closed Bomb Burning Rates for TS-3659 Propellant, as reported in "The High Energy Propellant Safety (HEPS) Program Highlights", CPIA Publication 456, Vol. I, p. 292, January 1987.
12. V. A. Veretennikov, A. N. Dremin and K. K. Shvedov, **Combustion, Explosion & Shock Waves** (English translation of **Fizika Goreniya i vzryva**), Vol. 5, No. 4, 1969, p. 342 (translation volume).
13. M. R. Baer and J. W. Nunziato, "A Multiphase Model for the Compressive Combustion of Ball Propellant", 1989 JANNAF Propulsion Systems Hazards Meeting, 21-24 February 1989, San Antonio, Texas.

14. T. Hsieh and K. Kim, "Numerical Simulation of Piston-Driven-Compaction Experiments for TS-3659 and WC-140 Propellants", 1989 JANNAF Propulsion Systems Hazards Meeting, 21-24 February 1989, San Antonio, Texas.
15. D. E. Kooker, "Predictions for the Piston-Driven-Compaction Experiment Based on a Transient Shock Wave Model", 1989 JANNAF Propulsion Systems Hazards Meeting, 21-24 February 1989, San Antonio, Texas.
16. C. F. Price, A. I. Atwood, H. P. Richter and T. L. Boggs, "Modeling the Behavior of Mechanically Stimulated Porous Beds", 1989 JANNAF Propulsion Systems Hazards Meeting, 21-24 February 1989, San Antonio, Texas.
17. A. M. Weston and E. L. Lee, "Modeling 1-D Deflagration to Detonation Transition (DDT) in Porous Explosives", **Eighth Symposium (International) on Detonation**, NSWC MP 86-194, pp. 914-925, 15-19 July 1985.

APPENDIX - SCHEMATIC DESCRIPTION OF MODELS

BAER (SNLA) [see Ref. 13]

- o Compressible solid phase.
- o Zero wall friction.
- o Equilibrium stress state, β_p , is fit to the combined dynamic data (PDC) and quasi-static compaction data (Elban, et. al.)
- o Does not account for stress deviators (each phase represented with a pressure).
- o Finite-rate porosity change based on "compaction viscosity" - leads to prediction of finite-thickness compaction wave.

Mass Source Term = Compressive Reaction + Grain Burning

$$\frac{\rho_s(\phi_s - \phi_s^0)}{\tau_H}$$

$\left[\begin{array}{l} \neq 0 \text{ only when } T_i \geq T^* \\ \text{heat transfer to cold solid} \\ \text{determines } T_i(t) \end{array} \right]$

Compressive reaction -

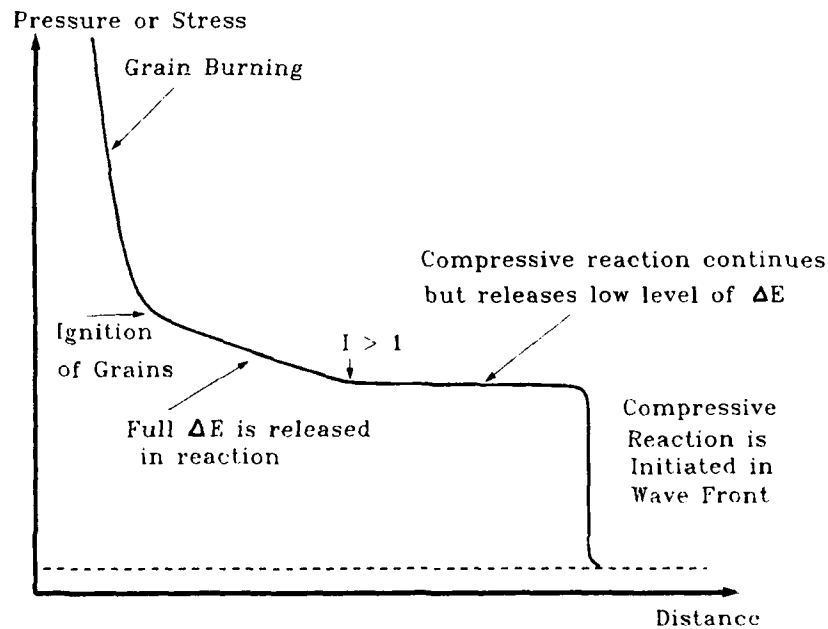
o $1 / \tau_H = \text{constant} * P_m^2$

o Energy released in reaction depends upon delay time " I ".

$$\Delta E = Q^* + (\Delta E_R - Q^*) H(I-1) \quad \text{where } H(I-1) = 1 \text{ when } I \geq 1.$$

o Delay time " I " is tracked along gas-phase streamlines, such that

$$D(I) / D(t_g) = 1 / \tau_{\text{delay}} \quad \text{where} \quad \tau_{\text{delay}}^{-1} = \text{constant} * P_m^2$$



HSIEH & KIM (NSWC) [see Ref. 14]

- o Incompressible solid phase.
- o Zero wall friction.
- o Equilibrium stress state is fit to quasi-static compaction data.
- o Does not account for stress deviators (hydrostatic solid stress and gas pressure only).
- o No rate-dependent resistance to porosity change ("compaction viscosity" = 0).
- o Drag force between solid and gas phases was neglected in Workshop computations.

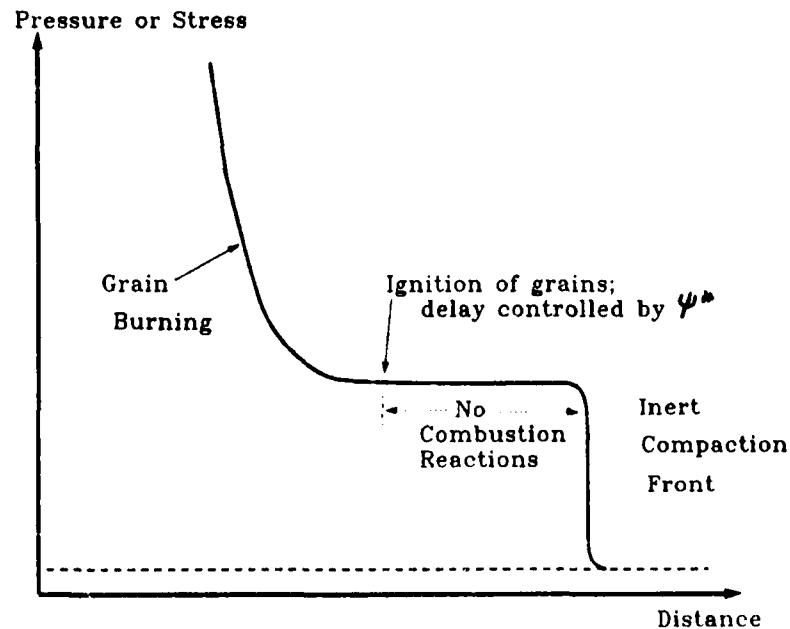
Uses GOUGH'S "XNOVAK" Code ----- with modifications

Mass Source Term = Grain Burning

- o Single step reaction releases full chemical energy of solid phase
- o Onset of this reaction is delayed until achieving ψ^* , where

$$\psi^* = \int_0^T \tau_i^2 dt, \quad \text{for each Eulerian control volume}$$

the value of ψ^* follows from Sandusky's correlation, $\tau_i^2 \Delta t = \text{constant} = \psi^*$.



KOOKER (BRL) [see Ref. 15]

- o Compressible solid phase.
- o Zero wall friction.
- o Equilibrium stress state is fit to quasi-static compaction data.
- o No explicit use of stress deviators (each phase represented with a pressure).
- o Instantaneous porosity adjustment (compaction viscosity = 0) to equilibrium stress state.
- o Compaction waves are shock waves with zero thickness (method-of-characteristics solution)
- o Compaction wave front induces small amount of reaction (produces gas-phase intermediate products)

$$\text{Mass Source Term} = \text{Gas-Phase Reaction} + \text{Grain Burning}$$

$$\left[\begin{array}{l} \neq 0 \text{ only when } T_i \geq T^* \\ \text{heat transfer to cold solid} \\ \text{determines } T_i(t) \end{array} \right]$$

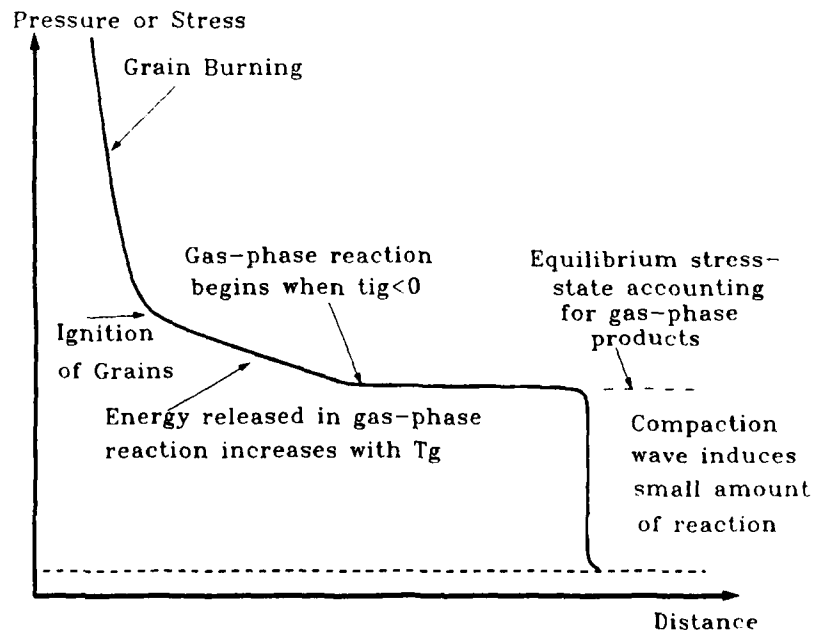
Gas-phase reaction "begins" with intermediate products from wave-induced reaction.

- o Reaction is delayed until $t_{ig} \ll 0$

$$D(t_{ig})/D(t_g) = -1, \text{ where } t_{ig}(0) = t_{ig}^0 \text{ comes from } P_m^2 \Delta t = \text{constant}$$

- o Amount of energy released is a function of gas-phase temperature, T_g

$$D(\Delta e_{gr})/D(t_g) = \text{constant} * \exp(-\text{constant} / T_g)$$

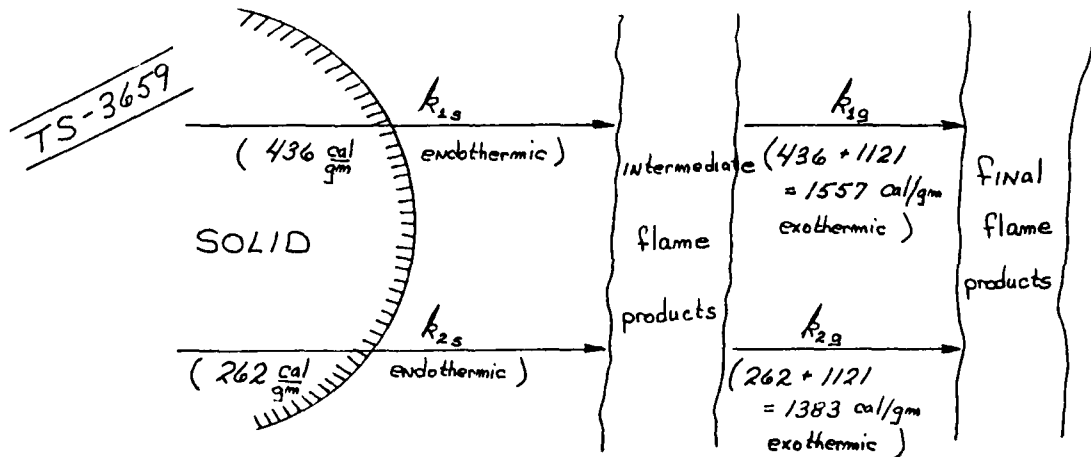


PRICE (NWC) [see Ref. 16]

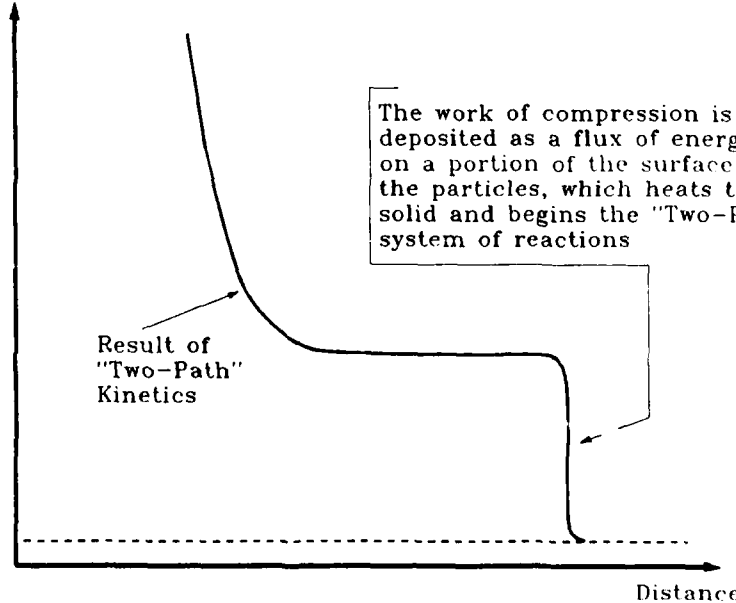
- o Compressible solid phase.
- o Accounts for wall friction.
- o Equilibrium stress state is fit to quasi-static compaction data.
- o Mixture stress tensor is a pressure, but intragranular stress is function of parameters called shear modulus, bulk modulus, etc. [At Workshop, reported radial stress = $0.6 * \text{mixture pressure}$.]
- o No rate-dependent resistance to porosity change ("compaction viscosity" = 0) other than inertial forces.

Heavily Modified Version of Joint Venture Two-Phase Flow Code (-- roots to Krier, et. al.)

No Artificial Distinction Between Ignition & Transient Combustion
All Reaction & Energy Release are Incorporated into "Two-Path Kinetics"



Pressure or Stress



WESTON (Brobeck/LLNL) [see Ref. 17]

- o Compressible solid phase.
- o Accounts for wall friction.
- o Equilibrium stress state is fit to quasi-static compaction data.
- o Extensive analysis based on stress deviators.
- o No rate-dependent resistance to porosity change ("compaction viscosity" = 0).

Modified "R-DUCT" Model

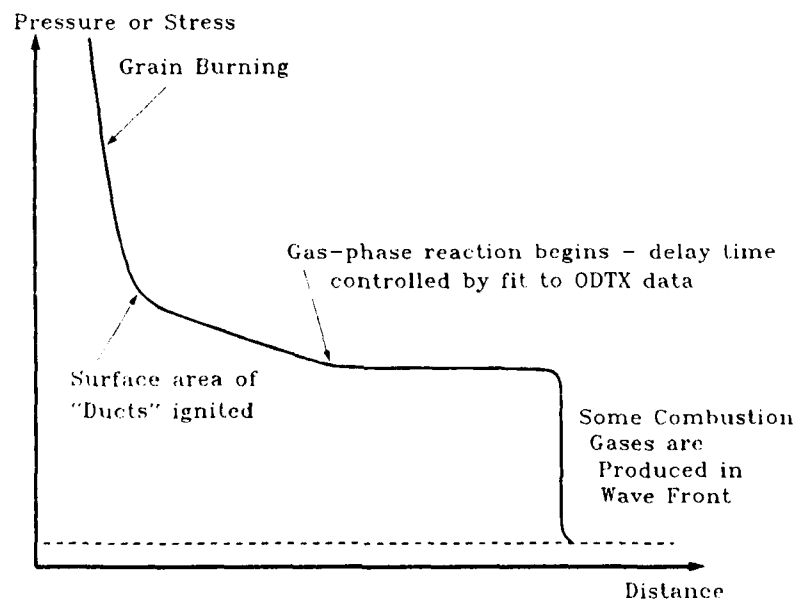
$$\text{Mass Source Term} = \text{Gas-Phase Reaction} + \text{Grain Burning}$$

$\left[\begin{array}{l} \neq 0 \text{ only when } T_i \geq T^* \\ \text{heat transfer to cold solid} \\ \text{determines } T_i(t) \end{array} \right]$

Gas-Phase Reaction -

- o Reaction releases full chemical energy of solid phase.
 - o Delay time before onset of reaction is controlled by parameters fit to "ODTX" data.
- plus
- o An additional reaction in the leading compaction front generates some gas, according to

$$\text{Production rate} = \text{constant} * \text{strength of wave} * \text{compaction rate at local cell}$$



No of Copies	Organization	No of Copies	Organization
(Unclass., unlimited) 12	Administrator	1	Commander
(Unclass., limited) 2	Defense Technical Info Center		US Army Missile Command
(Classified) 2	ATTN: DTIC-DDA Cameron Station Alexandria, VA 22304-6145		ATTN: AMSMI-RD-CS-R (DOC) Redstone Arsenal, AL 35898-5010
1	HQDA (SARD-TR) WASH, DC 20310-0001	1	Commander US Army Tank Automotive Command ATTN: AMSTA-TSL (Technical Library) Warren, MI 48397-5000
1	Commander US Army Materiel Command ATTN: AMCDRA-ST 5001 Eisenhower Avenue Alexandria, VA 22333-0001	1	Director US Army TRADOC Analysis Command ATTN: ATAA-SL White Sands Missile Range, NM 88002-5502
1	Commander US Army Laboratory Command ATTN: AMSLC-DL Adelphi, MD 20783-1145	(Class. only) 1	Commandant US Army Infantry School ATTN: ATSH-CD (Security Mgr.) Fort Benning, GA 31905-5660
2	Commander Armament RD&E Center US Army AMCCOM ATTN: SMCAR-MSI Picatinny Arsenal, NJ 07806-5000	(Unclass. only) 1	Commandant US Army Infantry School ATTN: ATSH-CD-CSO-OR Fort Benning, GA 31905-5660
2	Commander Armament RD&E Center US Army AMCCOM ATTN: SMCAR-TDC Picatinny Arsenal, NJ 07806-5000	1	The Rand Corporation P.O. Box 2138 Santa Monica, CA 90401-2138
1	Director Benet Weapons Laboratory Armament RD&E Center US Army AMCCOM ATTN: SMCAR-LCB-TL Watervliet, NY 12189-4050	(Class. only) 1	Air Force Armament Laboratory ATTN: AFATT/DLODL Eglin AFB, FL 32542-5000
1	Commander US Army Armament, Munitions and Chemical Command ATTN: SMCAR-ESP-L Rock Island, IL 61299-5000		<u>Aberdeen Proving Ground</u> Dir, USAMSAA ATTN: AMXSY-D AMXSY-MP, H. Cohen Cdr, USATECOM ATTN: AMSTE-TO-F Cdr, CRDEC, AMCCOM ATTN: SMCCR-RSP-A SMCCR-MU SMCCR-MSI
1	Commander US Army Aviation Systems Command ATTN: AMSAV-DACL 4300 Goodfellow Blvd. St. Louis, MO 63120-1798		
1	Director US Army Aviation Research and Technology Activity Ames Research Center Moffett Field, CA 94035-1099		

<u>No. Of Copies</u>	<u>Organization</u>	<u>No. Of Copies</u>	<u>Organization</u>
1	Commander Armament R&D Center ATTN: SMCAR-SCA-T, L. Stiefel Bldg. 455 Dover, NJ 07801-0001	1	Commander Army Missile Command Redstone Sci Inf Ctr ATTN: DOC SEC Bldg. 4484 Redstone Arsenal, AL 35898-5000
1	Commander US R&D Center ATTN: SMCAR-LCA-G, A.J. Beardell Dover, NJ 07801-0001	2	Commander Army Msl Command Redstone Sci Inf Ctr ATTN: AMSMI-RD-PR-S, S.P.D. Smith AMSMI-XO, F.E. Hart Redstone Arsenal, AL 35898-5000
1	Commander Armament R&D Center Scientific & Tech Div ATTN: SMCAR-TSS Bldg. 59 Dover, NJ 07801-0001	2	Director US Army Research Office ATTN: DRXRO-PP-LIB DEXTR-PP-LIB, D.M. Mann P.O. Box 12211 Research Triangle Park, NC 27709
1	Director Army Def Ammo Ctr & Sch ATTN: SMCAC-ASA (URC), A.H. Bausman Savanna, IL 61074	2	Commander Army Strategic Defense Command - Huntsville ATTN: DASD-H-MPL, A.B. Dumas BMDSC-AD-LIB, D.C. Sayles P.O. Box 1500 Huntsville, AL 35807
1	Commander Army Fgn Sci & Tech Ctr ATTN: CH, H.M. Sheinfeld 220 7th Street, NE Charlottesville, VA 22901	1	Commander White Sands Missile Range ATTN: Tech Lib White Sands Missile Range, NM 88002
1	Commander Army Laboratory Command Mat Tech Lab ATTN: SLCMT-IML-Tech Lib, M.M. Murphy Watertown, MA 02172	3	Commander Naval Air Sys Command ATTN: NAIR-32/931A, G.E. Kovalenko AIR 5004, S.N. Block (54042) AIR-5004-Tech Lib Washington, DC 20361-9300
1	Commander Army Mat Command ATTN: AMCSF, Safety Office 5001 Eisenhower Avenue Alexandria, VA 22333		

<u>No. Of Copies</u>	<u>Organization</u>	<u>No. Of Copies</u>	<u>Organization</u>
1	Commanding Officer Naval Explo Ord Dspl Fac ATTN: Lib Div Indian Head, MD 20640	2	Commanding Officer Naval Ship Weapon System Engineering Station ATTN: Code 5125, E.C. Kalstein Code 4V21 M.W. Walker Port Hueneme, CA 93043
2	Commanding Officer Naval Tech Intelligence Ctr ATTN: Code DS-311 4301 Suitland Road Washington, DC 20395-5020	2	Commander Naval Surface Weapons Center ATTN: Code G-20, J.L. East Code E231, Tech Lib Dahlgren, VA 22448
3	Commanding Officer Naval Ordnance Station ATTN: Code 5253, T.C. Smith Code 5246, Tech Lib Code OE-5, J.A. Hannum Indian Head, MD 20640	2	Commander Naval Surface Weapons Center White Oak Laboratory ATTN: Code K-22, R.J. Edwards Code E432, S. Happel 10901 New Hampshire Avenue Silver Spring, MD 20903
1	Superintendent Naval Postgraduate School ATTN: Code 1424, Libs Dir Monterey, CA 93943		
1	Chief Naval Research ATTN: Code 1132P, R.S. Miller 800 N. Quincy Street Arlington, VA 22217	7	Commander Naval Surface Weapons Center White Oak Laboratory ATTN: Code R-13 R.R. Bernecker S. Jacobs H.W. Sandusky D. Price B. Glancy K. Kim C.W. Dickinson 10901 New Hampshire Avenue Silver Spring, MD 20903
1	Commanding Officer Naval Research Lab ATTN: Code 2627 Washington, DC 20375		
1	Commander Naval Sea Systems Command ATTN: SEA-06H, M.R. Vanslyke Washington, DC 20362	1	Commanding Officer Naval Underwater Sys Gmd ATTN: 021312, Tech Lib Newport, RI 02840
1	Commander Naval Sea Systems Command ATTN: SEA-09B312, Tech Lib National Center Bldg. 3 Washington, DC 20362		

<u>No. Of Copies</u>	<u>Organization</u>	<u>No. Of Copies</u>	<u>Organization</u>
4	Commander Naval Weapons Center ATTN: Code 32738, A.O. Smith Code 3272, R.W. Feist Code 327B, R.F. Vetter Code 3431 China Lake, CA 93555	1	Commander AEDC ATTN: Tech Lib Arnold AFS, TN 37389
4	Commander Naval Weapons Center ATTN: Code 3891, A. Atwood H.P. Richter C. Price E. Lundstrom China Lake, CA 93555	1	Commander AFFTC ATTN: Tech Lib Stop 238 Edwards AFB, CA 93523
1	Commanding Officer Naval Weapons Station ATTN: Code 322, T.W. Lohrmann Concord, CA 94520	10	Commander AFRPL ATTN: DYC, D.P. Weaver MKPL, C.E. Merrill MKPB, D.I. Thrasher MKPA, J.L. Trout MKAS, J.H. Clark LKCP, J.W. Marshall DY, R.L. Geisler MKA MKP Tech Lib Edwards AFB, CA 93523
2	Director Navy Strat Sys Proj Ofc ATTN: SP-2731, J.E. Culver Tech Lib Br Hd Washington, DC 20376	1	Commander AFSC ATTN: DLX-T, R.E. Smith Andrews AFB Washington, DC 20334
1	Commander Operations T&E Force Atlantic ATTN: Tech Lib Norfolk, VA 23511	1	Commander AFWAL (GLISL) ATTN: Tech Rpts Sec Wright-Patterson AFB, OH 45433
1	Commander AAMRL ATTN: TH Wright-Patterson AFB, OH 45433		
1	Commander AD ATTN: ENMP, R.H. Rhode Eglin AFB, FL 32542	1	Commander ASD ATTN: YYEF, J.V. Braum Wright-Patterson AFB, OH 45433

<u>No. Of Copies</u>	<u>Organization</u>	<u>No. Of Copies</u>	<u>Organization</u>
1	Commander ESMC ATTN: ETR/RA, M. Brown Patrick AFB, FL 32925	1	Purdue University Aeronautics & Astronautics ATTN: J.R. Osborne Grissom Hall West Lafayette, IN 47907
1	Commander FTD ATTN: TQTA, A. Crowder Wright-Patterson, AFB OH 45433	1	Southwest Research Institute ATTN: H.J. Gryting P.O. Drawer 28510 San Antonio, TX 78284
1	Commander FTD ATTN: SDBP Wright-Patterson AFB, OH 45433	4	Lawrence Livermore National Laboratory ATTN: L. Lee, L324 M. Costantino, L324 A. Weston, L324 E. James, L324 P.O. Box 808 Livermore, CA 94550
1	Commander Ogden Alc ATTN: MANPA, A.J. Inverso Bldg. 1941 Hill AFB, UT 84056	6	University of California Los Alamos National Lab ATTN: Report Lib, R. Rabie J. McAfee, J960 B. Asay, J960 J. Dick, P952 J. Ramsay, J960 C. Forest P.O. Box 1663 Los Alamos, NM 87545
1	Commander SAC ATTN: NRI-STINFO Offutt AFB, NB 68113	1	University of Illinois at Urbana ATTN: H. Krier 144 ME Building Urbana, IL 61801
1	California Inst Technology Jet Propulsion Lab, Lib Op Gp ATTN: Lib Acqs/Standing Orders 4800 Oak Grove Drive Pasadena, CA 91103	1	University of Illinois at Urbana Engineering Exp Station ATTN: Doc Lib 1308 W. Green Street Urbana, IL 61801
1	IIT Rsch Inst ATTN: Doc Lib 10 W. 35th Street Chicago, IL 60616	1	AAI Corporation ATTN: Tech Lib P.O. Box 126 Hunt Valley, MD 21030
1	Pennsylvania State Univ. Applied Rsch Lab ATTN: K.K. Kuo 312 Mechanical Eng. Bldg. P.O. Box 30 State College, PA 16801		

<u>No. Of Copies</u>	<u>Organization</u>	<u>No. Of Copies</u>	<u>Organization</u>
1	Aerojet General Corp Sacramento Facility ATTN: Tech Inf Ctr P.O. Box 13222 Sacramento, CA 95813	1	General Dynamics Corp Pomona Division ATTN: Div Lib, MZ-4-20-CH LIB Mail Zone 6-20 P.O. Box 2507 Pomona, CA 91766
1	Aerojet Tactical Systems ATTN: R. Mironenko P.O. Box 13400 Sacramento, CA 95813	1	General Dynamics Corp Convair Div ATTN: U.J. Sweeney P.O. Box 85357 San Diego, CA 92138
1	Aerospace Corp ATTN: S.B. Crowe P.O. Box 92957 Los Angeles, CA 90009	1	General Elec Co Armament & Elec Sys Dept ATTN: Eng Lib Lakeside Avenue Burlington, VT 05402
1	Air Products & Chem, Inc. ATTN: C.E. Anderson P.O. Box 538 Allentown, PA 18105	1	Grumman Aerospace Corp Engineering Lab ATTN: H.B. Smith MS 101-35 S. Oyster Bay Road Bethpage, LI, NY 11714
1	ARINC Research Corp Annapolis Sci Ctr ATTN: R. Blair 2551 Riva Road Annapolis, MD 21401	1	Hercules, Inc. Aerospace Division Allegany Ballistics Lab ATTN: LIB P.O. Box 210 Cumberland, MD 21502
1	Atlantic Research Corp ATTN: Tech Inf Ctr 7511 Wellington Road Gainesville, VA 22065	2	Hercules, Inc. Bacchus Works ATTN: Library M/S H, C.F. Partridge MS-J12D, G. Butcher P.O. Box 98 Magna, UT 84044-0098
1	Boeing Company Kent Library ATTN: 8K-38 Lib Proc Supv Mail Stop 74-60 P.O. Box 3707 Seattle, WA 98124	1	Hercules, Inc. ATTN: Tech Inf Ctr, Bldg. A-100 P.O. Box 548 McGregor, TX 76657
1	Calspan Corp ATTN: V.M. Young P.O. Box 400 Buffalo, NY 14225		
1	Ford Aerospace and Comm Aeronutronic Div ATTN: Tech Inf Svc, DDC ACQS Ford & Jamboree Roads Newport Beach, CA 92658		

<u>No. Of</u> <u>Copies</u>	<u>Organization</u>	<u>No. Of</u> <u>Copies</u>	<u>Organization</u>
1	HI Shear, Corp AD-Tech Div ATTN: Eng Dir, D.E. Olander 2600 Skypark Drive Torrance, CA 90509	1	McDonnell Douglas Corp ATTN: R.D. Detrick P.O. Box 516 St. Louis, MO 63166
1	Hughes Aircraft Co Electro Optical & Data Sys Gp ATTN: B.W. Campbell Bldg. E1E110 P.O. Box 902 El Segundo, CA 90245	1	Morton Thiokol, Inc. Tech Staff, Aerospace Group ATTN: T.F. Davidson 3340 Airport Road Ogden, UT 84405
3	Lockheed Msl & Space Co Tech Inf Ctr ATTN: Reports Org 52-52, B. 201, Lockheed Huntsville Facility ORG 83-10, Bldg. 157-3W, C. Havlik Advanced Aeronautics, T. Harsha 3251 Hanover Street Palo Alto, CA 94304	1	Morton Thiokol, Inc. Elkton Div, Aerospace Group ATTN: D.J. McDaniel P.O. Box 241 Elkton, MD 21921
1	Ltv Aerospace & Def Co ATTN: LIB 3-58200 Mail Stop EM-08 P.O. Box 655907 Dallas, TX 75265-5907	1	Morton Thiokol, Inc. Wasatch Div, Aerospace Group ATTN: J.E. Hansen P.O. Box 524 Brigham City, UT 84302
1	Marquardt Co Sub Isc Def & Space Gp Inc ATTN: LIB P.O. Box 9104 Van Nuys, CA 91409	1	Morton Thiokol, Inc. Huntsville Div ATTN: H.H. Sellers Huntsville, AL 35807
1	Martin Marietta Corp Orlando Aerospace ATTN: MP-30 - TIC P.O. Box 5837 Orlando, FL 32855	1	Morton Thiokol, Inc. Longhorn Div ATTN: Tech Lib P.O. Box 1149 Marshall, TX 75670
1	Martin Marietta Corp Denver Aerospace ATTN: Rsch Lib 2655 P.O. Box 179 Denver, CO 80201	1	Olin Corp Ordnance Prods ATTN: M.R. Rhine P.O. Box 278 Marion, IL 62959
		1	Raytheon Co Missile Sys Div ATTN: J. Durben Hartwell Road Bedford, MA 01730

<u>No. Of Copies</u>	<u>Organization</u>	<u>No. Of Copies</u>	<u>Organization</u>
1	Rockwell International Rocketdyne Div ATTN: Tech Inf Ctr 6633 Canoga Avenue Canoga Park, Ca 91304	5	TRW Inc TRW Electronics & Defense Sector ATTN: R.C. Reeve, San Bernardino R.J. Christiansen, 01/2010 S/1930 C.M. Orr K. Fleeter, RI/1028 One Space Park Redondo Beach, CA 90278
1	Rockwell International Space Sys Gp ATTN: TIC-D201-300-AJ01 12214 Lakewood Blvd. Downey, CA 90241		
3	Sandia National Labs Mail Svc Sec ATTN: Lib 3141, J. Van Berkel M.R. Baer, MS 1513 J. Cummings, MS 1513 P.O. Box 5800 Albuquerque, NM 87185	1	United Technologies Corp Chemical Systems Div ATTN: Tech Lib P.O. Box 50015 San Jose, CA 95150-0015
1	Stone Engineering Company ATTN: Scty Off, D. Owens 805 Madison Street (STE 2C) Huntsville, AL 35801	1	United Technologies Corp Research Center ATTN: M.E. Donnelly 400 Main Street East Hartford, CT 06108
1	Sundstrand Corp ATTN: C.A. Hull P.O. Box 7003 4751 Harrison Avenue Rockford, IL 61125	1	Universal Propulsion Co ATTN: H.J. McSpadden Black Canyon Stage 1 Box 1140 Phoenix, AZ 85029
1	Talley Inds Arizona Inc ATTN: K. St. Clair P.O. Box 849 Mesa, AZ 85201	2	Natl Aeronautics & Space Admin George C. Marshall Space Flight Center ATTN: SA42, J.Q. Miller AS24D Marshall Space Flight Center, AL 35812
1	Textron, Inc. AVCO Rsch Lab Textron ATTN: L.T. Nazzaro 2385 Revere Beach Pkwy Everett, MA 02149	3	Natl Aeronautics & Space Admin Office of Management ATTN: Admin Div NHB-12, Lib Sec RTP-6, F.W. Stephenson Code DS, W.R. Frazier Washington, DC 20546
1	Textron Inc Bell Aerospace Co Div ATTN: L.M. Breslauer P.O. Box 1 Buffalo, NY 14240		

<u>No. Of Copies</u>	<u>Organization</u>
1	Natl Aeronautics & Space Admin Wallops Flight Center ATTN: Code 250.9, J.N. Foster Wallops Island, WA 23337
1	Natl Aeronautics & Space Admin Langley Research Center ATTN: MS-185, Tech Lib Hampton, VA 23665
1	Natl Aeronautics & Space Admin Lewis Research Center ATTN: D. Morris 21000 Brookpark Road Cleveland, OH 44135
1	Natl Aeronautics & Space Admin Scientific Tech Inf Fac ATTN: Accessioning Dept P.O. Box 8757 Baltimore-Washington Intl Airport, MD 21240

USER EVALUATION SHEET/CHANGE OF ADDRESS

This laboratory undertakes a continuing effort to improve the quality of the reports it publishes. Your comments/answers below will aid us in our efforts.

- 1. Does this report satisfy a need? (Comment on purpose, related project, or other area of interest for which the report will be used.) _____
- 2. How, specifically, is the report being used? (Information source, design data, procedure, source of ideas, etc.) _____
- 3. Has the information in this report led to any quantitative savings as far as man-hours or dollars saved, operating costs avoided, or efficiencies achieved, etc? If so, please elaborate. _____
- 4. General Comments. What do you think should be changed to improve future reports? (Indicate changes to organization, technical content, format, etc.) _____

BRL Report Number _____ Division Symbol _____

Check here if desire to be removed from distribution list. _____

Check here for address change. _____

Current address: Organization _____
Address _____

-----FOLD AND TAPE CLOSED-----

Director
U.S. Army Ballistic Research Laboratory
ATTN: SLCBR-DD-T (NEI)
Aberdeen Proving Ground, MD 21005-5066

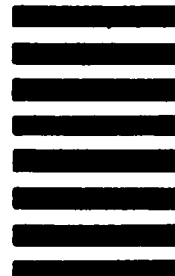


NO POSTAGE
NECESSARY
IF MAILED
IN THE
UNITED STATES

OFFICIAL BUSINESS
PENALTY FOR PRIVATE USE \$300

BUSINESS REPLY LABEL
FIRST CLASS PERMIT NO. 12062 WASHINGTON D. C.

POSTAGE WILL BE PAID BY DEPARTMENT OF THE ARMY



Director
U.S. Army Ballistic Research Laboratory
ATTN: SLCBR-DD-T (NEI)
Aberdeen Proving Ground, MD 21005-9989